Appendix F

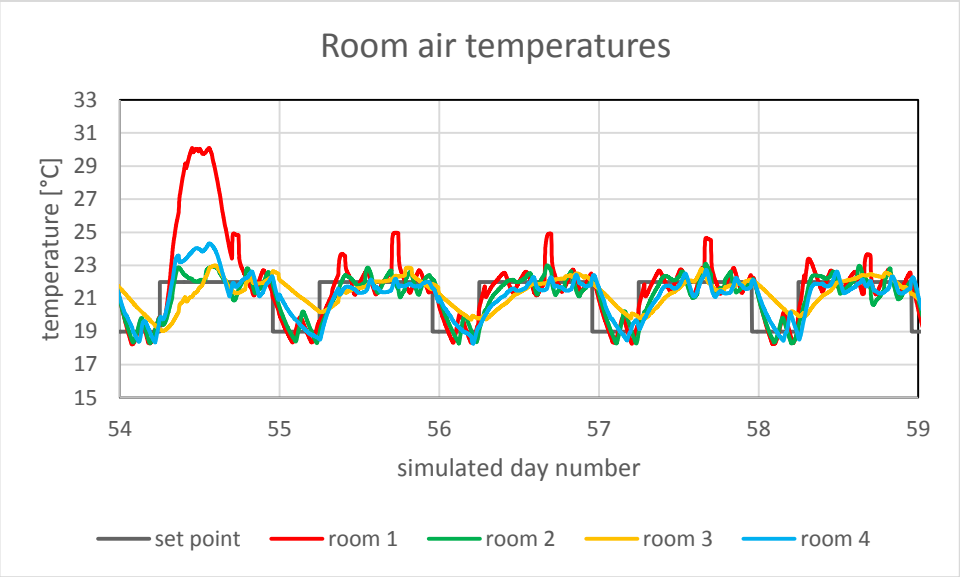

Evaluation of a baseline test on the OPSYS test rig

Energy and Climate

Søren Østergaard Jensen

DANISH TECHNOLOGICAL INSTITUTE

Title: Evaluation of a baseline test on the OPSYS test rig

Prepared by: Danish Technological Institute, Gregersensvej 1, DK-2630 Taastrup
Energy and Climate

Author: Søren Østergaard Jensen, Danish Technological Institute
Contact: Søren Østergaard Jensen, sdj@teknologisk.dk

April 2018
1st printing, 1st edition, 2018

Front page: The air temperatures in the four rooms of the building during five days of the baseline test

Preface

The present document is part of the documentation of the *Underfloor heating and heat pump optimization* project financed by the Danish Energy Agency through the EUDP programme, project no. 64014-0548.

The purpose of the document is to investigate how well the OPSYS test rig can emulate the conditions in a heat pump installation in a single-family house.

Participants in the work:

Søren Østergaard Jensen, Danish Technological Institute
Tomasz Minto, Aalborg University
Karsten Jørgensen Bang, Danish Technological Institute

Table of content

1 Introduction

The OPSYS test rig is described in Appendix A, while the software including the house model on the test rig pc is described in Appendix B-D. The present Appendix focuses on how well the test rig can create the desired conditions during a test. Furthermore, the measurements from the test rig is compared with the annual simulation model, which also has been created in the project as described in Appendix D. The reason for the latter comparison is to evaluate if the test rig and the annual simulation produce similar results. The tests carried out on the test rig are in real-time, which means that only shorter tests can be carried out while parametric studies can be carried out with the fast annual simulation model. Thus, the idea is that only special tests determined by the annual simulation program are carried out on the test rig in order to test these in a more realistic environment.

A so-called baseline test is evaluated in the following.

The baseline test is emulating the traditional control of a heat pump connected to an underfloor heating system. This means that the telestats (valves of the underfloor heating system) are individually on/off controlled, and the forward temperature from the heat pump is controlled based on the ambient temperature and a heating curve in the controller of the heat pump. The forward temperature is determined as a linear dependency of the ambient temperature, which in the baseline test was chosen to be:

ambient temperature	forward temperature
-15°C	50°C
20°C	25°C

The house model is configured as a Danish house from the 1970's (see Appendix C) with an annual space heating demand of 16,904 kWh and an annual electricity demand of 4,877 for the heat pump (using the simplified model of the heat pump described in Appendix D). No domestic hot water production was included in the test.

During the daytime, the set point for the air temperature of the rooms is 22°C as this is the typically preferred indoor temperature in Denmark. During the night the set point is set back to 19°C. The periods for the two set points are:

22°C: 6 am-11 pm
19°C: 11 pm-6 am

The simulation on the test rig pc forwards the following to the physical test rig:

- the ambient temperature of the given time
- the brine temperature of the given day
- the position of the telestats
- the return temperature of the four underfloor heating circuits

The test rig returns the following to the simulation program on the test rig pc:

- the volume flow rate in the four underfloor heating circuits
- the forward temperature from the heat pump to the underfloor heating circuits

The test was carried out for the simulated period: February 14th (day 45) to March 6th (day 65), i.e. three weeks as both days are included. Two other periods of the year are investigated in Appendix G, where the main focus was to create energy flexibility with the test rig and the annual simulation model. Thus, different control strategies compared to the ones investigated in the present Appendix are tested in Appendix G.

2 Evaluation of the baseline test

Figure 2.1 shows the ambient temperature during the baseline test in the test rig. The ambient temperature fluctuated between -15°C and 6.5°C. The aimed temperature of the brine during the same period is shown in figure 2.2. The desired brine temperature comes from Appendix C page 14-15. The aimed temperature of the brine inclined from 0.07°C to 0.86°C during the considered period. Figures 2.15 and 2.16 show how well the aimed temperature of the brine was reached.

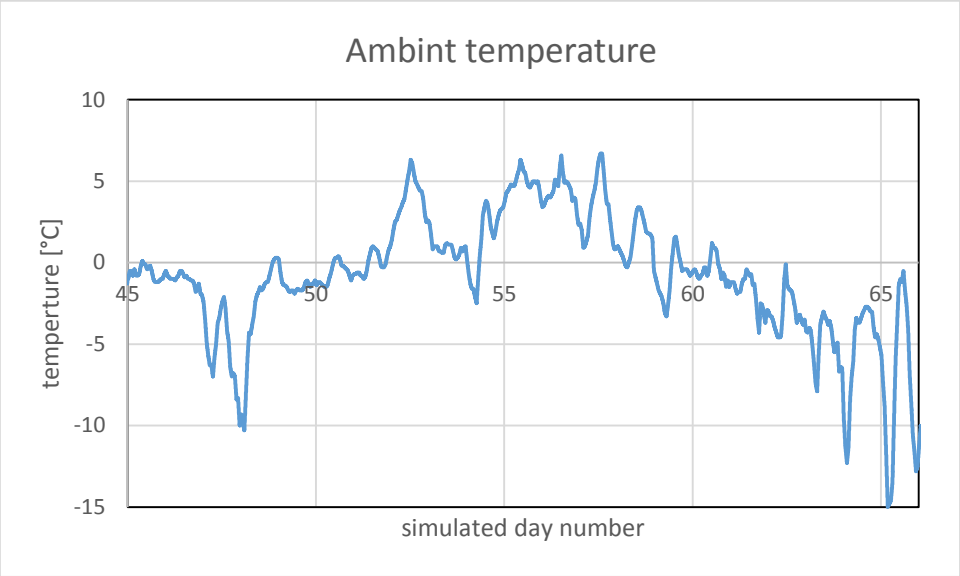

Figure 2.1. The ambient temperature during the period tested in the OPSYS test rig.

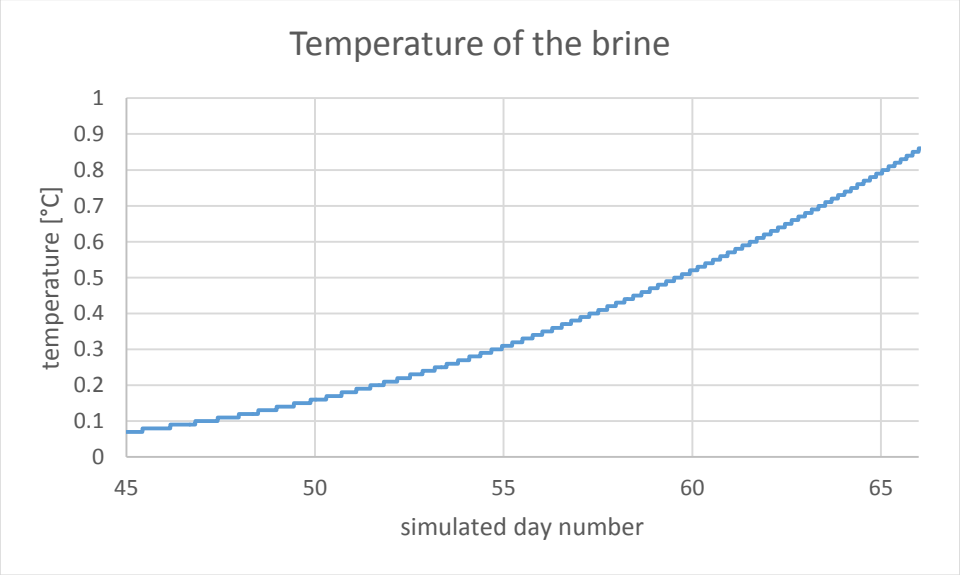

Figure 2.2. The aimed temperature of the brine to the heat pump during the same period as in figure 2.1.

The aim is to obtain realistic conditions in both the test rig and the annual simulation program. This is investigated in the following.

2.1 Introduction

The main purpose of a heating system is to obtain comfortable room air temperatures in a house. The simulated house is simplified to consist of four rooms – see Appendix A, C, and D. The set point of the room air temperatures is as already explained in the former chapter, 22°C during the day (as this is the most common temperatures in Danish houses) with a setback to 19°C during the night. Figure 2.3 shows the room air temperatures of the four rooms and the set point during the baseline test. During the day, the temperature of room 1 is sometimes very high. This is caused by solar radiation entering this room – see also figures 2.4 and 2.5. The low temperatures during the second night were caused by a need to increase the pressure in the brine circuit of the test rig. After this, a valve was accidentally positioned wrongly, so that the heat pump could not start for some hours. This is dealt with later in chapter 3.

Due to the many days, figure 2.3 is difficult to interpret. Therefore, figures 2.4 and 2.5 show two five-day periods: figure 2.4 includes the highest ambient temperature of the baseline test, and figure 2.5 includes the lowest ambient temperature of the baseline test.

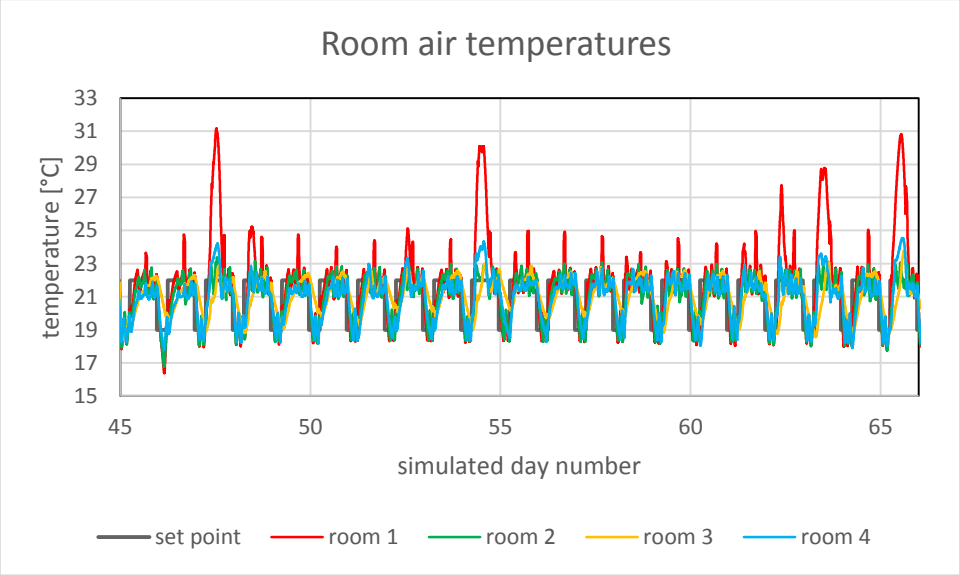

Figure 2.3. The room air temperatures during the baseline test.

The internal gains from persons and appliances are described in Appendix C. One main internal gain is the heat produced when cooking. This gain increases the room air temperature of room 1 as seen in figure 2.4. This cooking peak is further dealt with in Appendix G.

The underfloor heating in room 1, 2, and 4 is light weight (wooden surface) while the underfloor heating in room 3 (the bathroom) is heavy (concrete with tiles on top) – see Appendix D. This difference in thermal mass is clearly seen in figures 2.4 and 2.5. The yellow line (room 3) shows a very different pattern when compared to the three other rooms. The air temperature in room 3 decreases more slowly when the night setback starts and the increase after the night set back is also slower than for the rest of the rooms. The patterns of the air temperatures of the three rooms shown in figures 2.4 and 2.5 seem very realistic. This is further elaborated on in section 2.6.

As the whole test period is too difficult to interpret on, the chapter will mainly concentrate on one five-day period. The chosen period includes the days 54-58 (February 23th-28th - both inclusive) – i.e. the period shown in figure 2.4. The reason for choosing this period is that the ambient temperature fluctuates between 0 and 7°C, which is rather typical for the Danish winter situation.

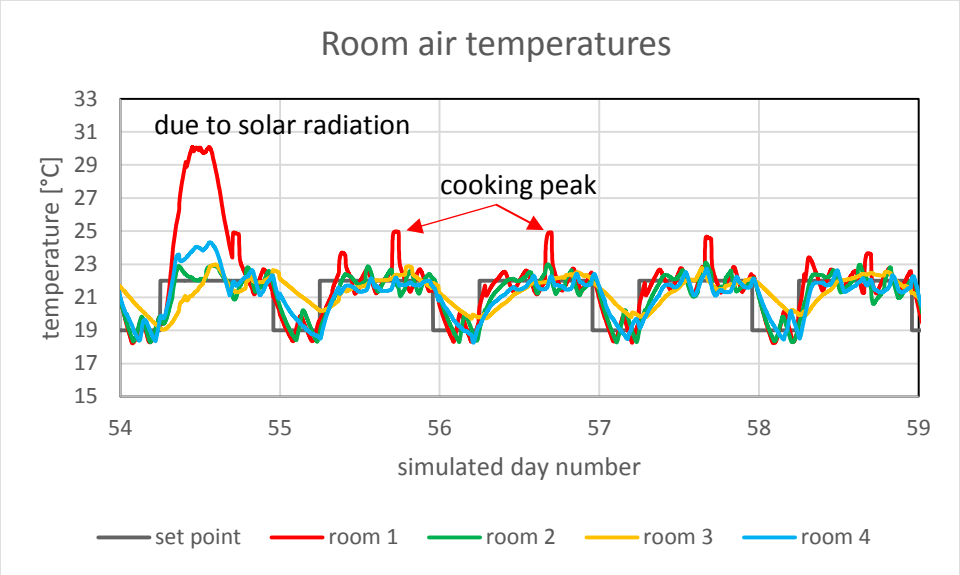

Figure 2.4. The room air temperatures during five days of the baseline test.

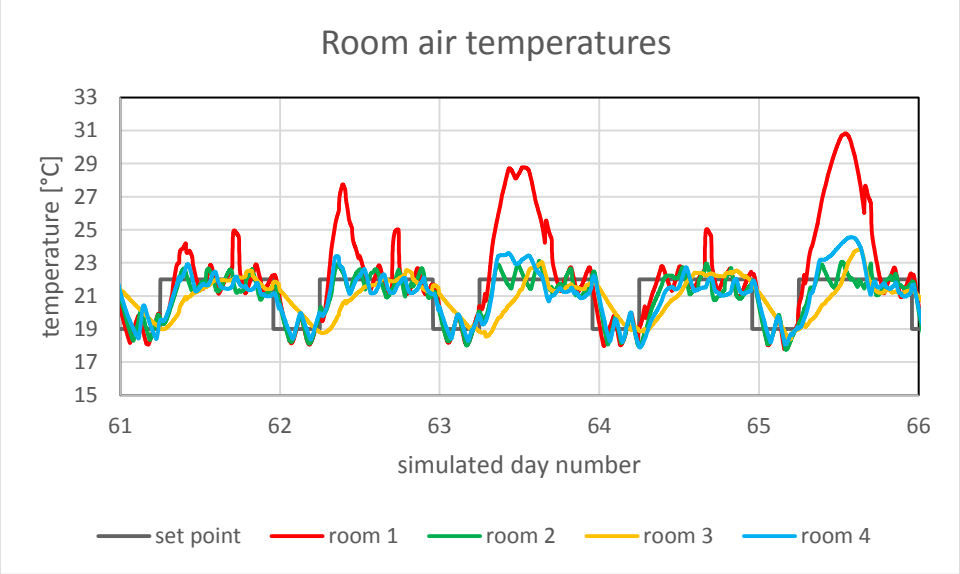

Figure 2.5. The room air temperatures during five days of the baseline test.

Figures 2.6-10 show the mass flow rates through the heating system for the chosen five-day period. Figure 2.6 shows the total mass flow rate, which also is the mass flow rate though the heat pump. Figures 2.7-10 show the mass flow rate in each of the underfloor heating circuits of the four rooms. Room 1 has four circuits, so the values in figure 2.7 should be multiplied by four in order to obtain the total mass flow rate to room 1. Room 2 has three circuits, so the values in figure 2.8 should be multiplied by three in order to

obtain the total mass flow rate to room 2. Rooms 3 and 4 have only one circuit each, so figures 2.9 and 2.10 show the total mass flow rate to these two rooms.

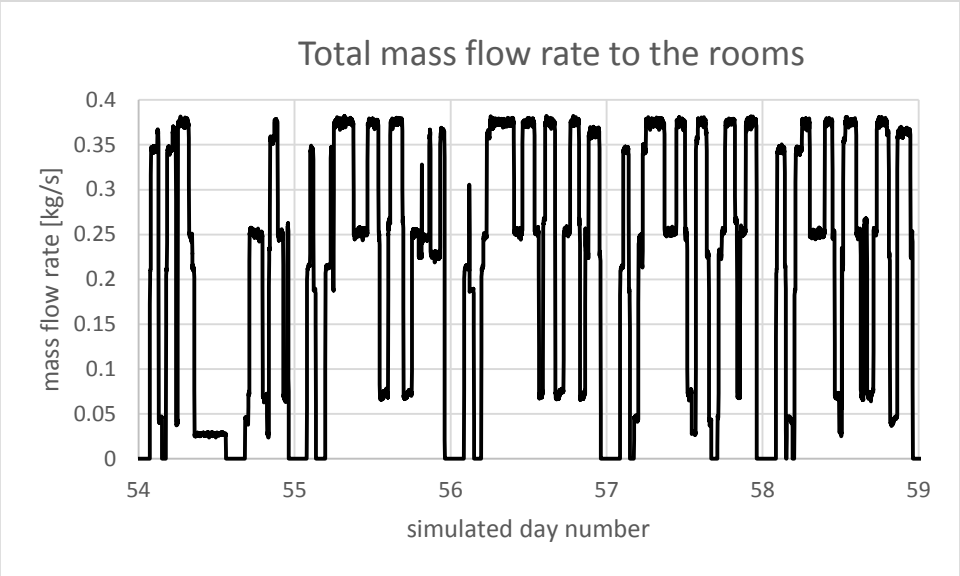

Figure 2.6. Total mass flow rate to the rooms.

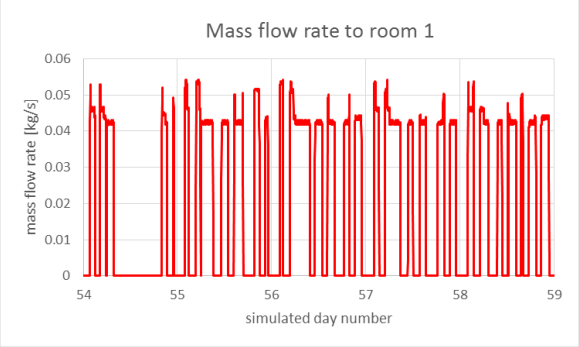

Figure 2.7. One fourth of the mass flow rate to room 1.

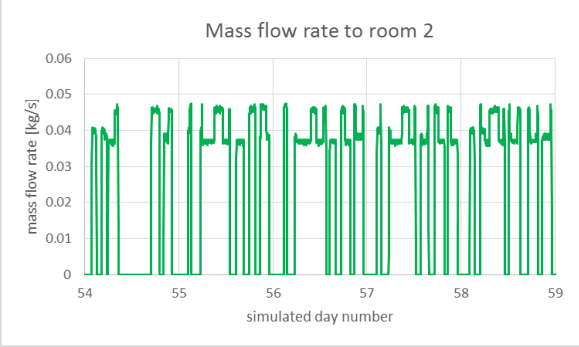

Figure 2.8. One third of the mass flow rate to room 2.

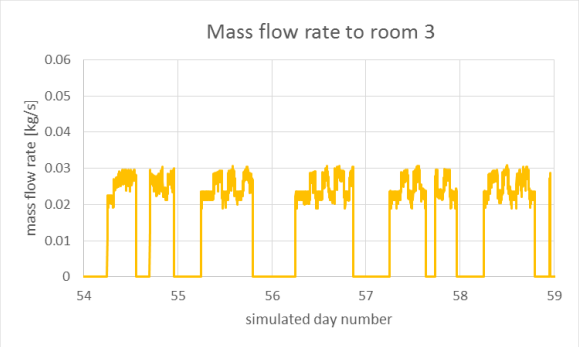

Figure 2.9. The mass flow rate to room 3.

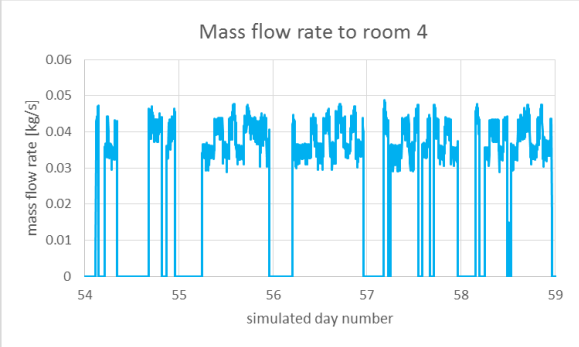

Figure 2.10. The mass flow rate to room 3.

As expected, figure 2.6 shows a rather fluctuating pattern of the total mass flow rate through the system. The reason for this fluctuation is that the opening of the four valves (telestats) is uncoordinated. They open and close independently of each other. They are only controlled by the set points and the actual air temperatures in the four different rooms. One purpose of the OPSYS project was to investigate if a less fluctuating behav-

iour of the flow rate through the system would lead to a higher total annual COP (efficiency) of the system. This is dealt with in Appendix E.

From figures 2.7-10, it is seen that the mass flow rates through the circuits of the underfloor heating in the four rooms are not fixed values. This is due to the pressure loss of the different circuits. If there is only a flow rate to one room, then the flow rate to this room will be higher than if there are flow rates to other rooms as well. This is shown more clearly in figure 2.11:

black circle:	the flow rate to room 1 is higher when there are no flow rate to other rooms. As soon as a flow rate to room 2 starts, the flow rate to room 1 will decrease with around 13 %. The same goes for room 2.
purple circle:	the flow rate to room 3 (and room 4) decreases when the flow rate to room 1 is switched on.

This phenomenon is also seen in real houses, so the test rig emulates the patterns of the flow rates correctly.

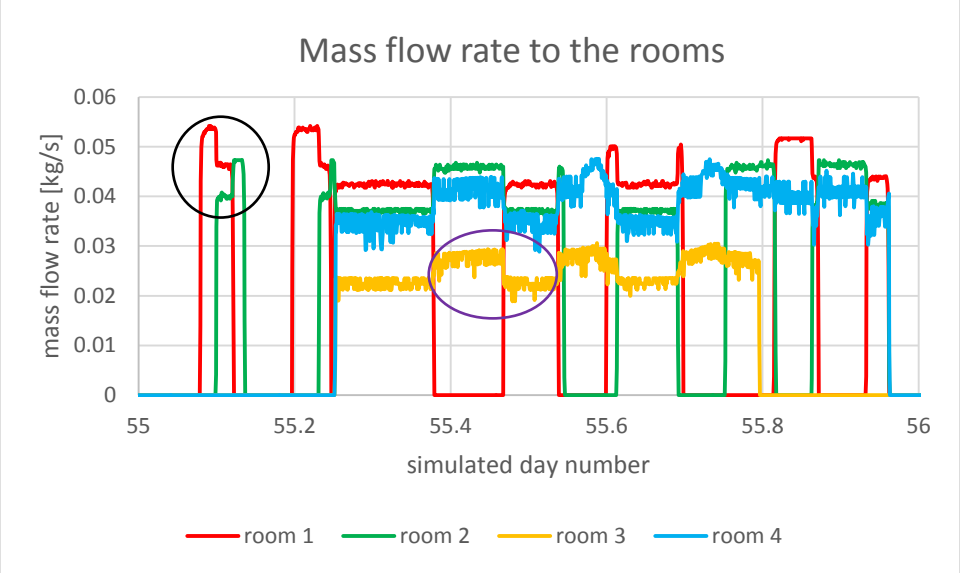

Figure 2.11. Total mass flow rates to the rooms during one day of the baseline test.

In the following, different features of the test rig will be investigated one by one using the data from the baseline test. In section 2.6, measured values will also be compared with the same values, which have been obtained with the annual simulation program.

2.2 Forward temperature

The forward temperature of the heat pump is as described in Appendices A and D manipulated in order to be able to test specific periods of the year and to optimize the forward temperature. The latter in order to optimize the annual COP of the system – please refer to Appendix E. In the baseline test, the virtual ambient temperature sent to the heat pump is the actual ambient temperature of the considered period of the year. When optimizing the forward temperature, the control calculates a virtual ambient temperature, which makes the heat pump deliver heat at the desired forward temperature.

With the applied heating curve of the heat pump, the forward temperature is 50°C at an ambient temperature of -12°C and 25°C at an ambient temperature of 20°C. Figure 2.12 shows a comparison of the obtained forward temperature (measured with the Trend BMS system) with the forward temperature calculated using the heating curve of the heat pump as mentioned above. Figure 2.12 shows that the measured forward temperature fluctuates around the desired forward temperature. The reason for this fluctuation is the thermal inertia of the test rig and the heat pump as seen more clearly in figure 2.13, which shows only one day and includes the total mass flow rate of the system.

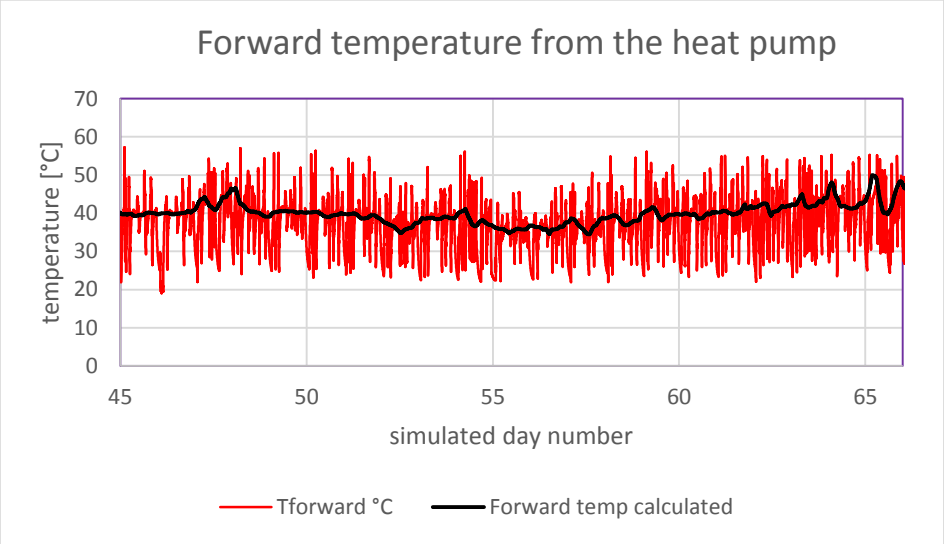

Figure 2.12. The forward temperature - measured and desired - of the baseline test.

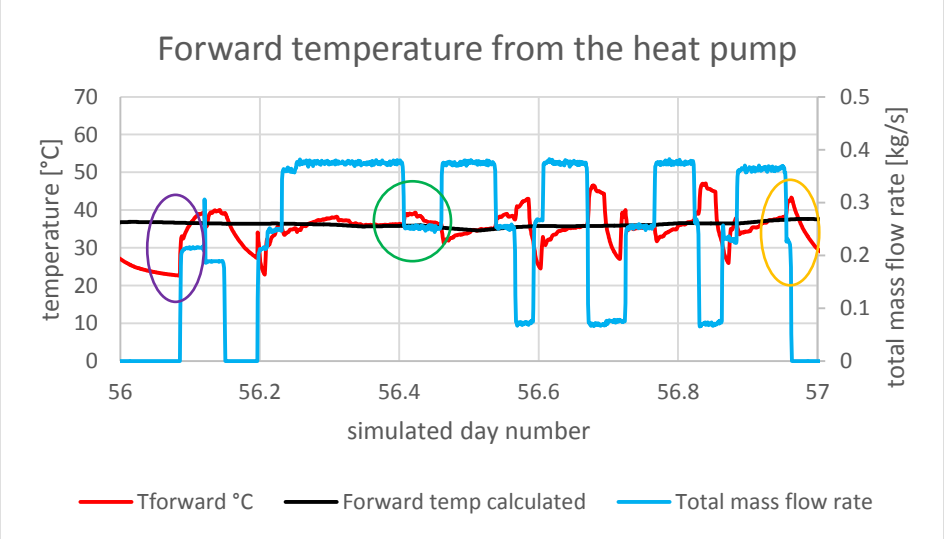

Figure 2.13. The forward temperature - measured and desired - of the baseline test.
Purple circle: when the heat pump starts up, it takes a while before the forward temperature reaches the desired level, but overshoots at first
Green circle: when the flow rates is reduced, the forward temperature goes slightly up, and the opposite occurs when the flow rate increases
Orange circle: when the heat pump stops, the forward temperature decreases slowly to the temperature of the room where the test rig is situated

The patterns of the forward temperature seen in figures 2.12 and 2.13 are also present in real systems due to the thermal inertia of the heat pump and the heat emitting system. It takes a while to heat up and cool down the heat pump and the heat emitting system when the mass flow rates change. However, the test rig may heat up slightly quicker than a real system due to the less water in the heat emitting circuits of the test rig compared to a real underfloor heating system. This has not been investigated in the present project.

2.3 Temperature of the brine

The evaporator of the heat pump cools the brine, thus, a heating element is needed to obtain the correct temperature of the brine to the heat pump. This is shown in figure 2.14.

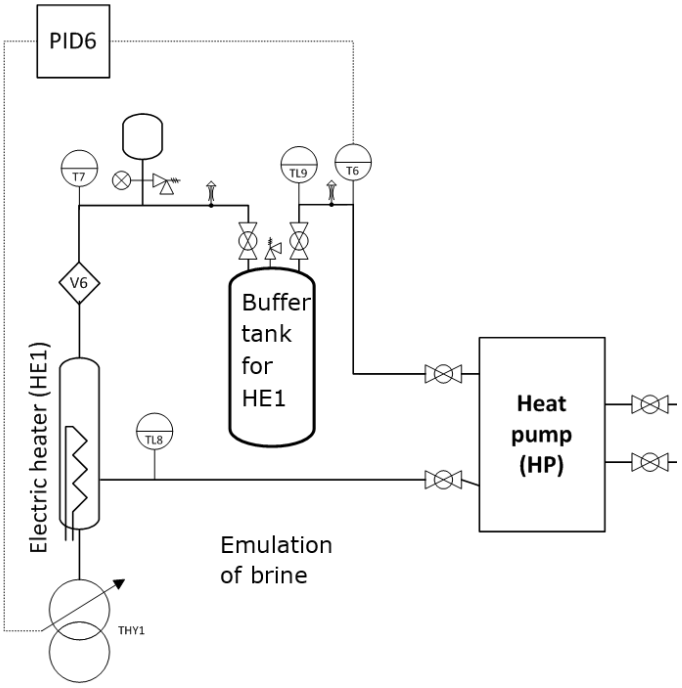

Figure 2.14. The brine circuit of the test rig. The figure is part of figure 2.3 of Appendix A showing the whole test rig.

The heating element HE1 can be modulated continuously between 0 and 7 kW by a thyristor (THY1). THY1 is controlled by a PID controller (PID6) based on a combination of T7 and T6. Despite the continuous control of the heating element, the temperature of the brine fluctuated rather much. A buffer tank (HE1) was, therefore, subsequently installed in the circuit between the heating element and the heat pump. Figure 2.15 shows a comparison between the measured and the desired (from figure 2.2) temperature of the brine.

When the flow stops in the brine circuit, the measured temperature goes rather quickly towards the temperature of the laboratory, in which the test rig is situated – i.e. around 20°C. When the heat pump is running, the temperature of the brine fluctuates around the desired temperature (named "calc temp" in figure 2.15). This is shown more clearly in figure 2.16, where the flow rate in the brine circuit is shown as well. Figure 2.16 shows the same day as figure 2.13.

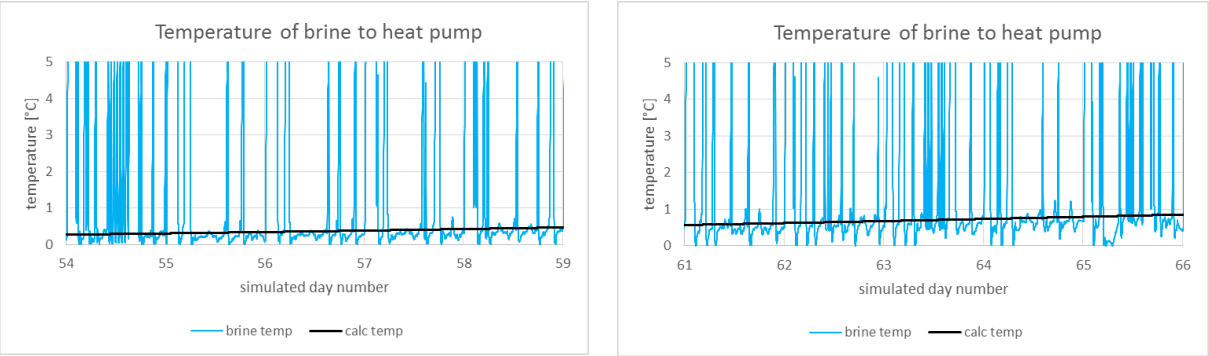

Figure 2.15. The measured and aimed temperature of the brine to the heat pump.

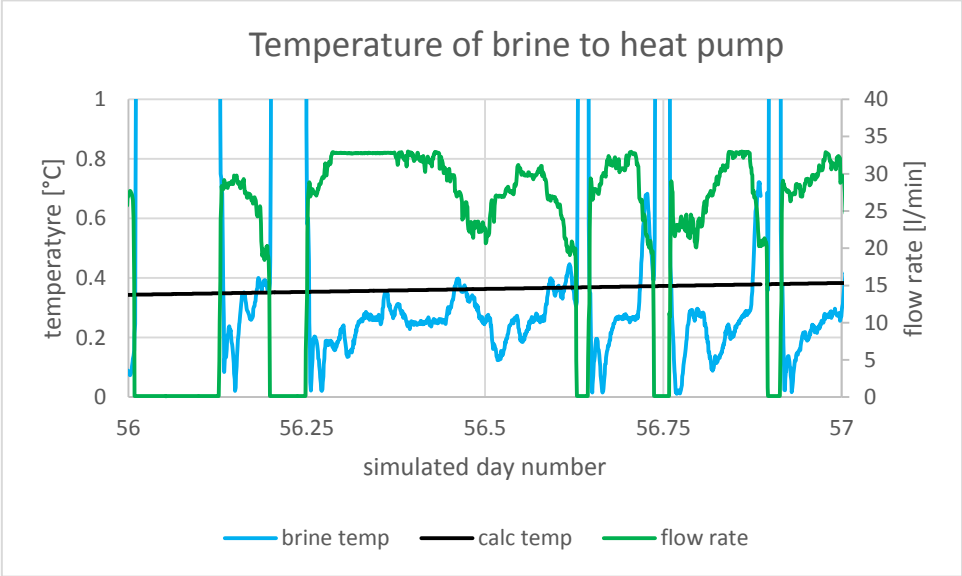

Figure 2.16. The measured and aimed temperature of the brine to the heat pump as well as the flow rate in the brine circuit for one day.

Figure 2.16 shows a fluctuation around the desired temperature of around ±0.3 K when there is a flow rate in the brine circuit. This is acceptable when considering the layout of the brine circuit – figure 2.14 – with the heating element located outside the large thermal mass – i.e. the buffer tank HE1. A less fluctuating behaviour of the brine temperature can be obtained by locating the heating element in the buffer tank. However, if the heat pump has been standing still for a while, the temperature of the buffer tank will increase, and the time for obtaining stable conditions will increase as well. Therefore, cooling of the buffer tank should possibly also be considered, even though both cooling and heating of the same tank is asking for troubles.

2.4 Return temperatures from underfloor heating

The underfloor heating of the four rooms is emulated by four heat exchangers connected to the cooling system in the laboratory at Energy and Climate, Danish Technological Institute. The return temperature is simulated by the house model of the test rig, while PID controllers of the BMS system of the test rig control the valves on the cold side of the heat exchangers in order to obtain the desired return temperatures from the underfloor heating circuits as seen in figure 2.17.

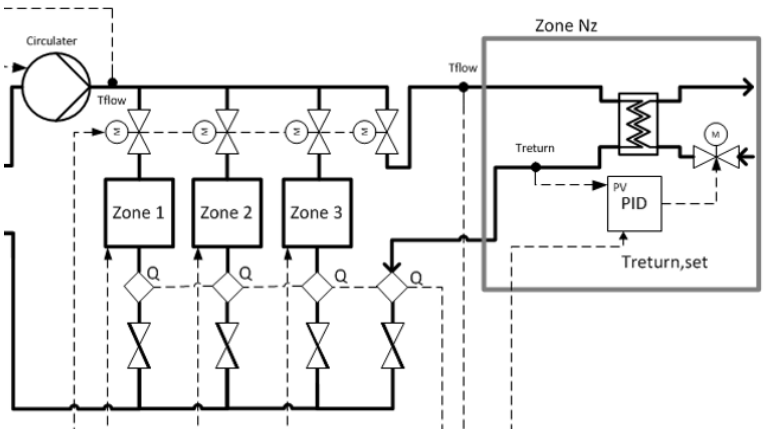

Figure 2.17. The four heat exchangers emulating the four rooms of the test rig. The figure is part of figure 2.4 in Appendix A, which shows the whole test rig.

Figure 2.18 shows a comparison between the desired return temperatures simulated by the house model of the test rig and the return temperatures measured at the test rig. The flow rates to the rooms are also shown.

Figure 2.18 shows a surprisingly good agreement between the simulated and the measured return temperatures from the floors although the tuning of the PID controllers can be rather tricky. Differences between the simulated and the measured return temperatures only occur when there is no flow to a room. This is due to the different thermal inertia of the test rig compared to the modelled thermal inertia of the house model. However, as the measured return temperatures quickly get identical to the simulated return temperatures as seen in figure 2.19, when the flow starts again, this deviation is of no importance.

On day 54, there is a period without flow to room 1, 2, and 3. This is due to solar radiation as seen in figure 2.4, where especially the air temperature of room 1 gets very high due to incoming solar radiation through the windows.

Room 3 shows a strange behaviour around noon of day 54. The return temperature is very fluctuating. This is shown in close-up below figure 2.18. The fluctuation is determined by the house model. This figure shows that the test rig is able to follow such fast fluctuations.

2.4.1 Cooling of heat exchangers emulating heat emitters of the underfloor heating system

The cooling of the four heat exchangers in the test rig is done using the central cooling plant in the laboratory at Energy and Climate, Danish Technological Institute. However, as this cooling plant is utilized for several purposes, the temperature of the brine may change during a test in the test rig. A buffer tank and a heat exchanger are, therefore, located in-between the four heat exchangers in the test rig and the central cooling system as seen in figure 2.20. The set point of the buffer tank is fixed in the simulation program on the test rig, while a PID controller of the BMS system in the test rig controls a valve in order to maintain the temperature of the buffer tank at the desired temperature level.

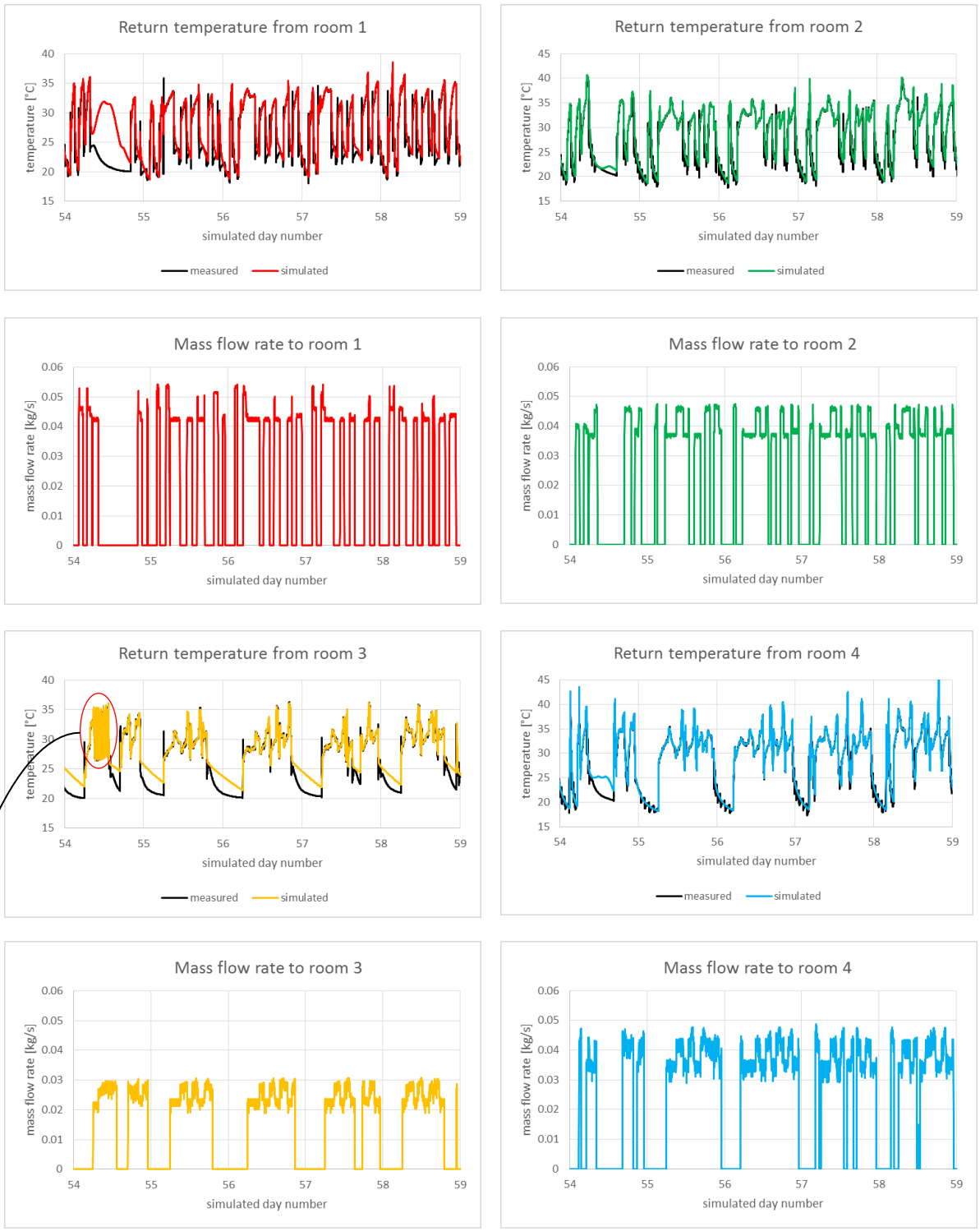

Figure 2.18. Simulated and measured return temperatures as well as measured mass flow rates.

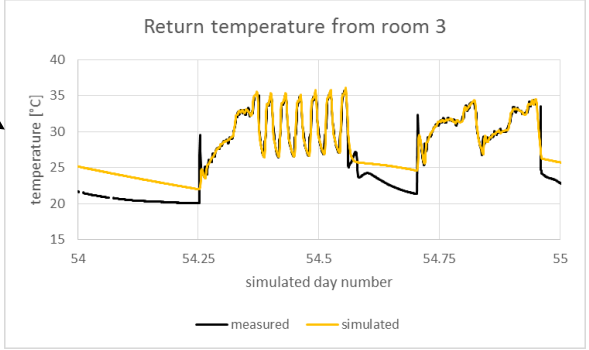

The fast fluctuations determined by the house model of the test rig are nicely followed by the test rig. The reason for the fluctuations is that the heat demand of the house is low due to solar radiation. Thus, the heat pump is on/off controlled during this period (in order to follow the actual low heat demand) as opposed to continuously controlled as seen in figure 2.33.

Figure 2.19. Simulated and measured return temperatures as well as measured mass flow rates for one day.

Figure 2.21 shows the temperature of the cold buffer tank during the baseline test. The desired temperature was 17°C. The temperature of the buffer tank fluctuates ±3-4 K around 17°C due to different heat loads of the four heat exchangers of the test rig as seen in figure 2.22, where the temperature of the cold buffer tank is compared with the total mass flow rate in the underfloor heating system. However, the temperature is suffi-

ciently stable in order to create the desired return temperatures from the four heat exchangers as shown in figures 2.18 and 2.19.

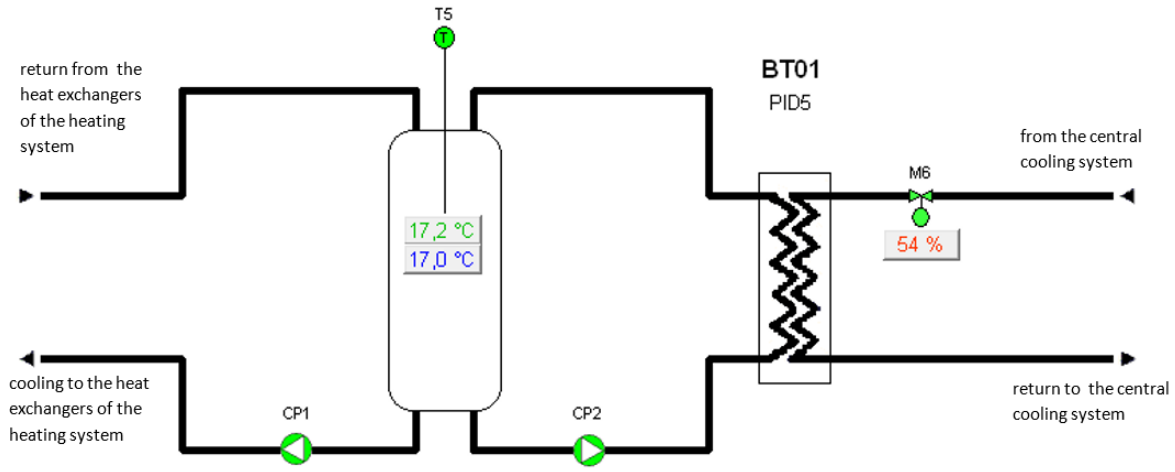

Figure 2.20. Screen shot of the cooling part of the test rig from the BMS system of the test rig.

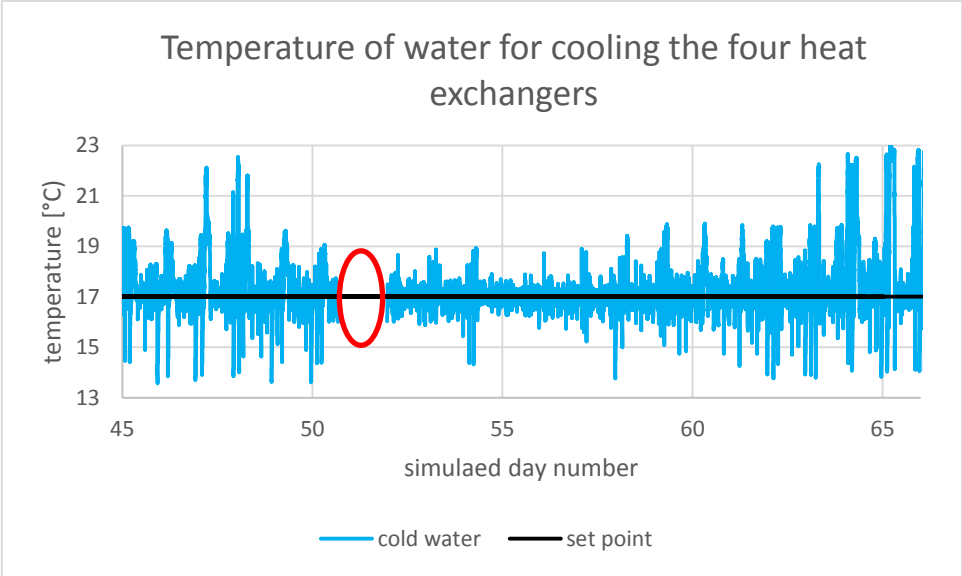

Figure 2.21. The temperature of the cooling buffer tank during the baseline test.

Figure 2.21 shows a hole in the measured data from the test rig (red oval). This is due to the fact that the GUI of the Trend BMS called 963 stopped during this period. The 963 is responsible for the screens showing the different parts of the BMS on the test rig – e.g. figure 2.20, but it is not responsible for the running of the test rig – only for setting up tests. However, 963 also logs measurements from the test rig in special purpose files. The missing measured data from the test rig is not a problem in the here described test as focus in the following is on the periods: days 54-58 and days 61-65.

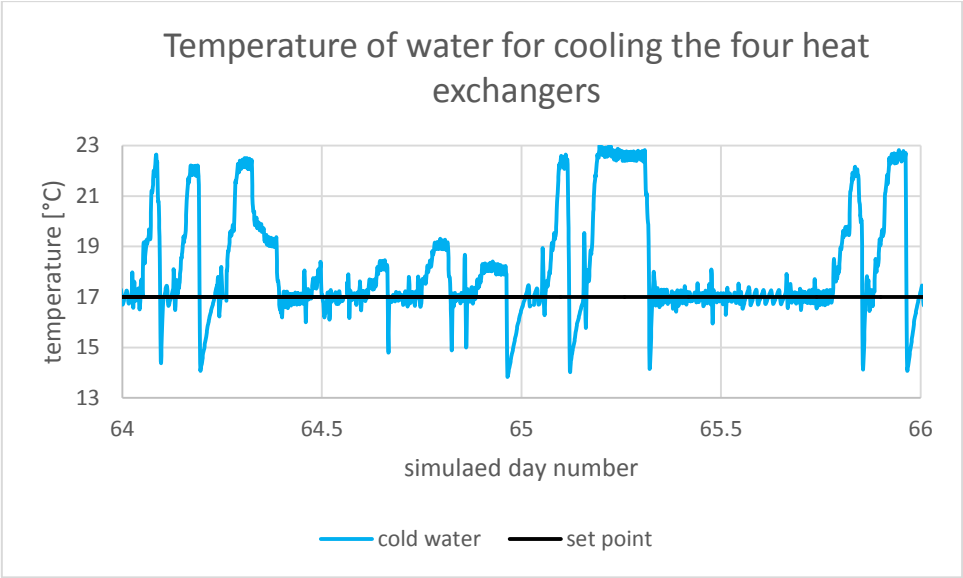

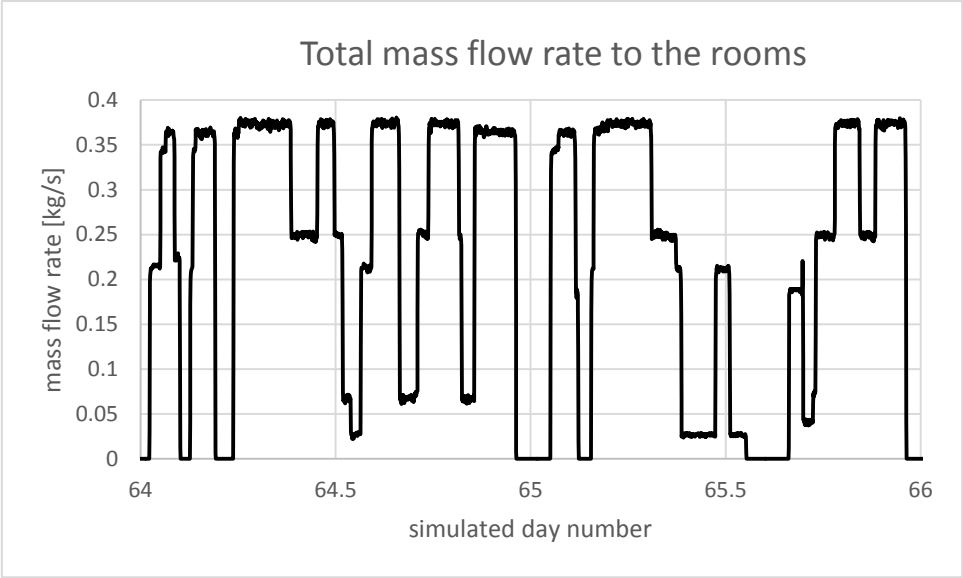

Figure 2.22. The temperature of the cooling buffer tank and the total mass flow rate through the underfloor heating system of the test rig during two days.

2.5 Flow rates of underfloor heating

The set point of the room air temperatures was 22°C during the day and 19°C during the night. However, it is not possible to make the room air temperatures follow the set point precisely. In the baseline case, the hysteresis of the room air temperatures was ±0.5 K meaning that the room air temperatures were allowed to fluctuate ±0.5 K around the set point. As an example, the fluctuation around the set point is seen in figure 2.4, but the fluctuation seems to be more than ±0.5 K. The reason for this is the reaction time of the telestats in the floor heating system. It takes some time from the simulation program asks a telestat to open or close until the telestat reacts, and if the heat pump is stopped and it has to be started up, it takes some time for this to react as well. Furthermore, the time from fully closed to fully open is for the chosen telestats 300 seconds (and the same from fully open to fully closed) as the valves are operated by wax motors, where the wax

melts and solidifies. This is seen in figure 2.23. In this case, the valve was fully open after 10.5 minutes while it closed within 4 minutes.

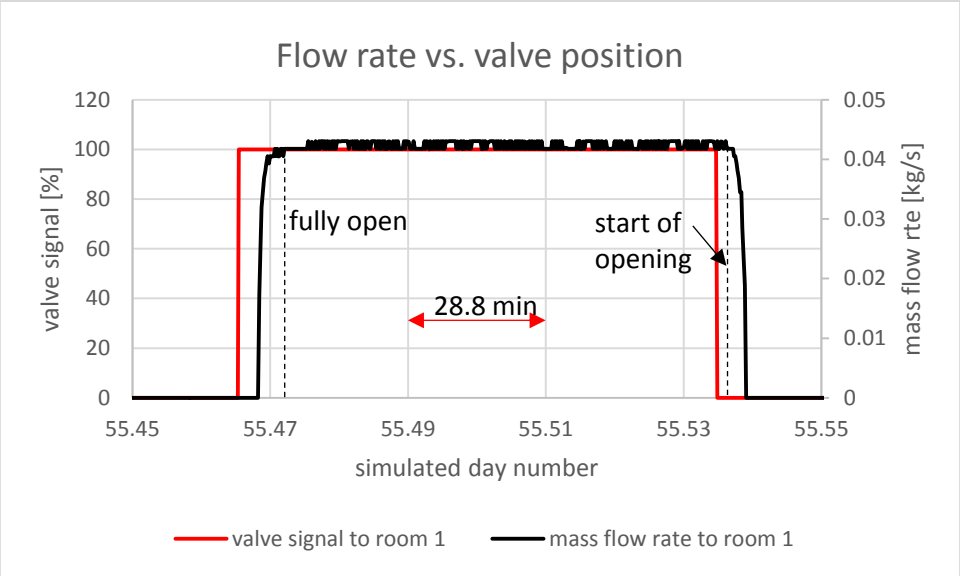

Figure 2.23. The time of start and stop of (one fourth of) the flow rate to room 1 compared with the signal given by the thermostats of the room. The graph is based values every 15 seconds.

The above behaviour is similar to a real heating system.

2.6 Comparison with the annual simulation program

The OPSYS platform consists of two main tools for investigation of the combined control of heat pumps and heat emitting systems. The two tools are the OPSYS test rig and the fast annual simulation program. As the two tools are able to investigate identical control strategies in different ways – one as hardware in the loop and one completely virtual, it is important to investigate if the two tools give comparable results.

Several measured values from the baseline test are compared with the same values from the annual simulation program for the same period of the year. The results from comparisons of other periods are shown in Appendix G, where a period in January and a period in April are investigated.

The forward temperature is already compared in figures 2.12 and 2.13. The reason for the difference is that the annual simulation program does not consider the thermal capacity of the heat pump as the model of the heat pump is very simplified as described in section 2.6.1 and in Appendix D.

The temperature of the brine has also already been compared - in figures 2.15 and 2.16. The measured brine temperature is more fluctuating than the simulated temperature. This is partly due to the way the temperature of the brine is maintained in the test rig, and partly due to the fact that the simulation does not consider the heat flow from the soil to the brine. Such stable conditions as simulated in figures 2.15 and 2.16 will hardly be possible in a real installation.

The return temperature does not need to be compared as it is the same house model, which is utilized at the test rig and in the annual simulation problem, so that the calculation procedure of the return temperature is identical in the two cases. The return temperature is of course not identical at identical time steps as the forward temperature (figures 2.12 and 2.13) and the flow rates differ from the two cases. The latter is compared in figure 2.24.

Figure 2.24. The measured and the simulated mass flow rates to the rooms. For room 1, one fourth of the flow rate and for room 2, one third of the flow rate.

Figure 2.24 shows a rather good agreement between the flow rates in the test rig and the flow rates anticipated by the annual simulation program. The measured flow rates have slightly faster fluctuations than the simulated flow rates. The reason for this is that the measured flow rates are logged each minute, while the simulated flow rates are logged every ten minutes. The measured flow rates to rooms 1 and 2 are slightly higher than the simulated flow rates, while the opposite is the case for rooms 3 and 4. The reason for this is that it is difficult to adjust the pressure losses of the heat exchangers in the test rig to obtain identical flow rates compared to the flow rates of the annual simulations.

Figure 2.24 shows that the annual simulation also captures the changes in the flow rate to one room dependent on wether there is flow to the other rooms or not – as discussed in connection with figure 2.11.

Figure 2.25 shows a comparison between the total measured mass flow rate and the simulated mass flow rate in the system. Figure 2.25 shows that the flow rates occur more or less at the same time in both the test rig and in the annual simulation. The total flow rate of the simulation is, however, slightly lower than in the test rig.

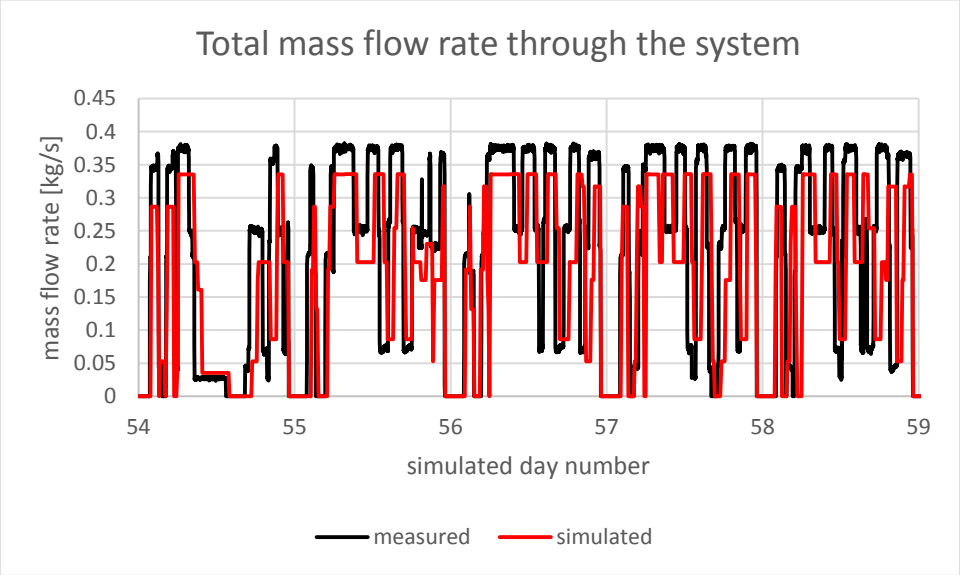

Figure 2.25. Total mass flow from the test rig (measured) and the annual simulation (simulated).

Figure 2.26 shows the same situation as figure 2.23, but from the annual simulation program. From figure 2.26, it seems that the opening of the valve happens gradually over a period of ten minutes. However, this not correct. The graduate opening of the valve seen in figure 2.26 is caused by the ten-minutes time steps of the simulation. However, a period of 300 seconds = 5 minutes from fully closed to fully open and vice-versa, is included in the simulation program, but this cannot be seen in the simulation program due to the ten-minutes time steps. A ten-minutes rest period for the heat pump after a switch off is also included in the annual simulation program in order to reduce the number of switch on/off sequences of the heat pump. This is a normal feature of heat pump controls in order to decrease wear and tear of the heat pump.

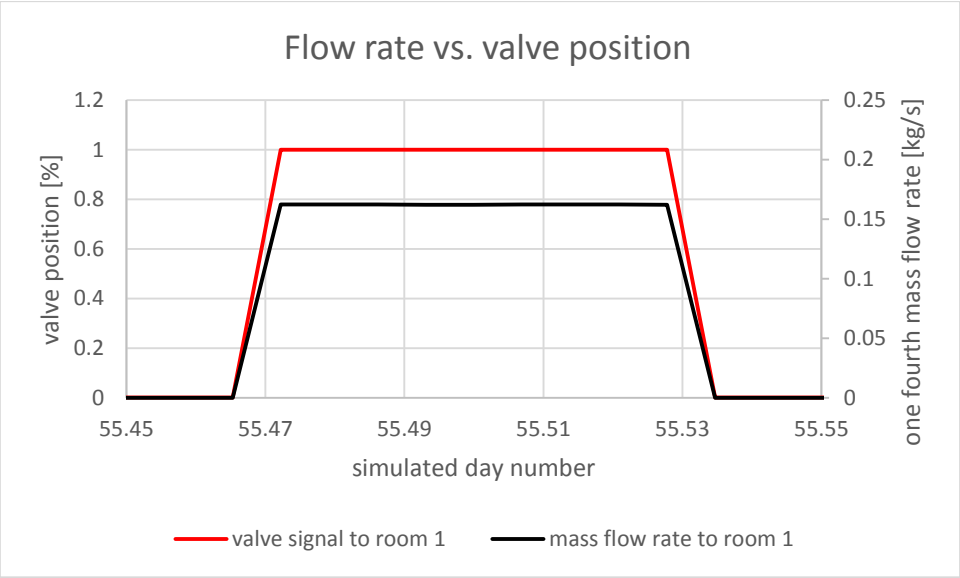

Figure 2.26. The incorrect switch on/off period of the valves in the annual simulation.

2.6.1 Comparison of room air temperatures and power to the heat pump

In the former sections the forward temperature, the brine temperature, and the return temperatures as well as the flow rates have been investigated, and they seem to be well represented by the two OPSYS tools. However, for the owner of a heat pump installation, it is more important that the two tools estimate the room air temperatures and the power consumption of the heat pump correctly. This is investigated in the following.

Results from the test rig will be compared with results from the annual simulation program. The comparison includes both periods and single days.

Figure 2.27 shows a comparison of the period also shown in figure 2.4, which was the "warmest" period of the baseline test, while figure 2.28 shows a comparison of the coldest period of the baseline test – also shown in figure 2.5. Figures 2.29 and 2.30 show a more detailed comparison of two days: one with clear sky conditions and one with overcast conditions.

Figures 2.27-30 and Appendix G show a very good agreement between the air temperatures of the rooms obtained with the test rig and the annual simulation. Furthermore, the patterns of the room air temperatures seem very realistic. In chapter 3 (and in Appendix G (section 4.2)), it is shown that due to the low thermal capacity of the test rig, it only takes one day or less after the start-up of the test rig before it has obtained stable conditions, which are comparable with the annual simulation program.

Figures 2.29 and 2.30 show that it takes some time for the room air temperatures to reach 22°C after the end of the night setback at 6 am. This could be due to a too small heat pump as the heat pump of the annual simulation program often runs at its maximum capacity as seen in figure 2.32. However, the heat pump of the test rig (which is bigger) seldom runs as its maximum capacity (3.5 kW) as also seen in figure 2.32. Therefore, the reason for the slow heating-up of the house is mainly due to the inertia of

the underfloor heating system. This is also illustrated by the pattern of the air temperature of the bathroom (room 3), which has a more heavier floor as opposed to the other rooms. It would, therefore, be beneficial for the comfort of the bathroom if the duration of the night setback was different from the other rooms. However, this is not possible with the typical control of heat pump installations as the night setback is handled at the level of the heat pump and not at the level of the different rooms. Thus, many may prefer not to utilize the possibility of night setback, which may lead to a higher heat demand of the house, however dependent on the insulation level and the thermal mass of the house. Different set points and variable durations of the night setback for the different rooms are easy to implement in the controllers investigated in this project as the investigated controllers have direct access to the thermostats of the rooms – please see Appendix E.

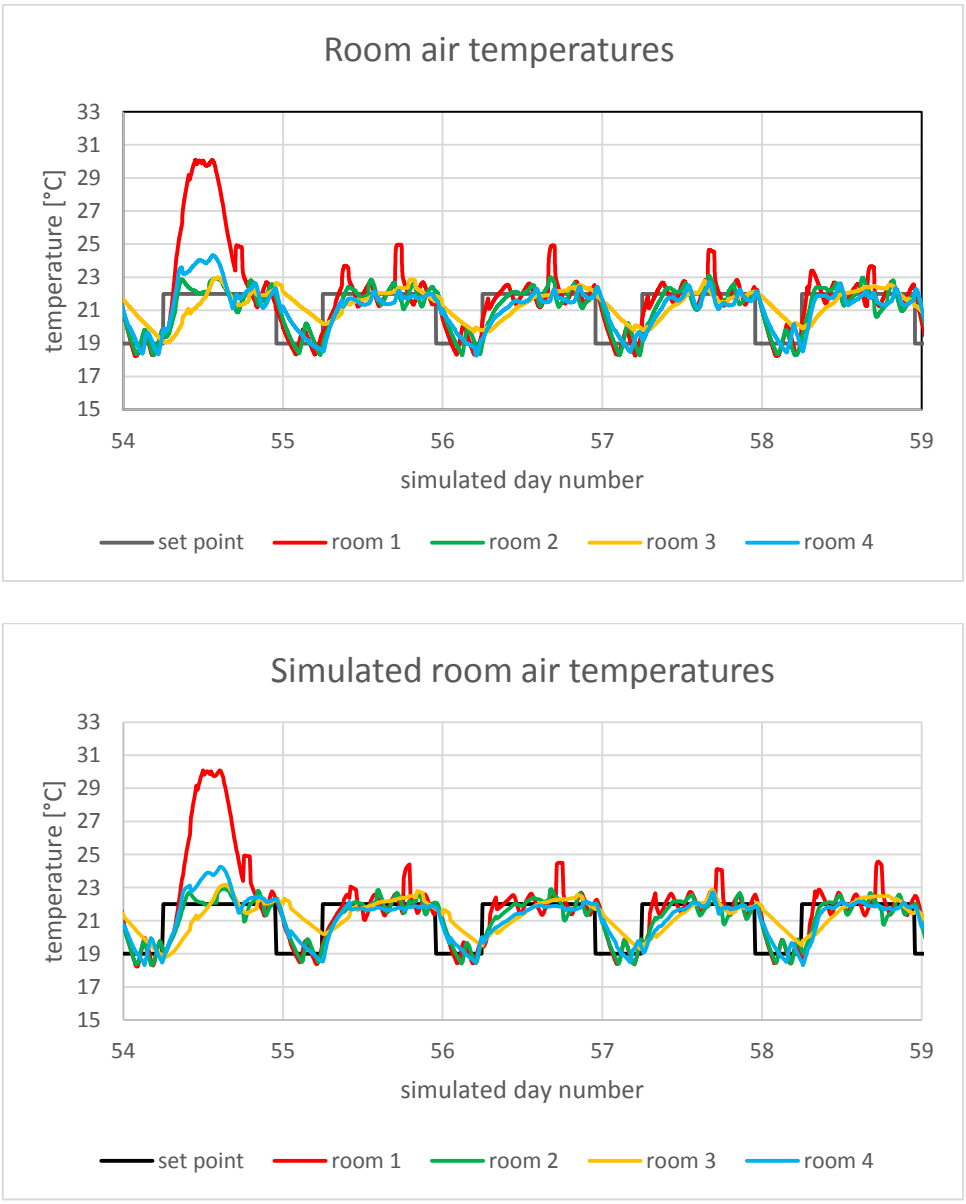

Figure 2.27. Comparison of air temperatures in the four rooms between the test rig (top) and the annual simulation program (bottom) for a five-day period of the baseline test.

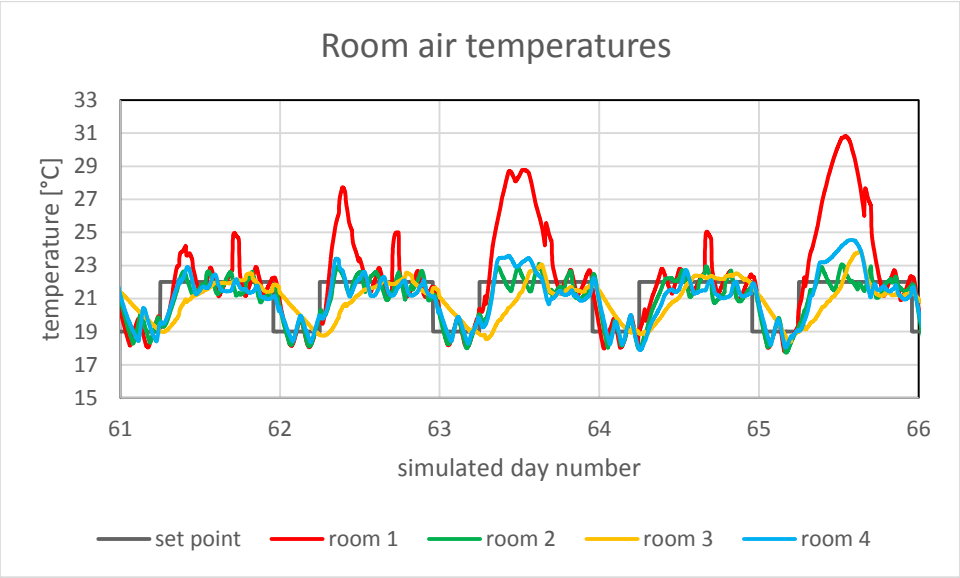

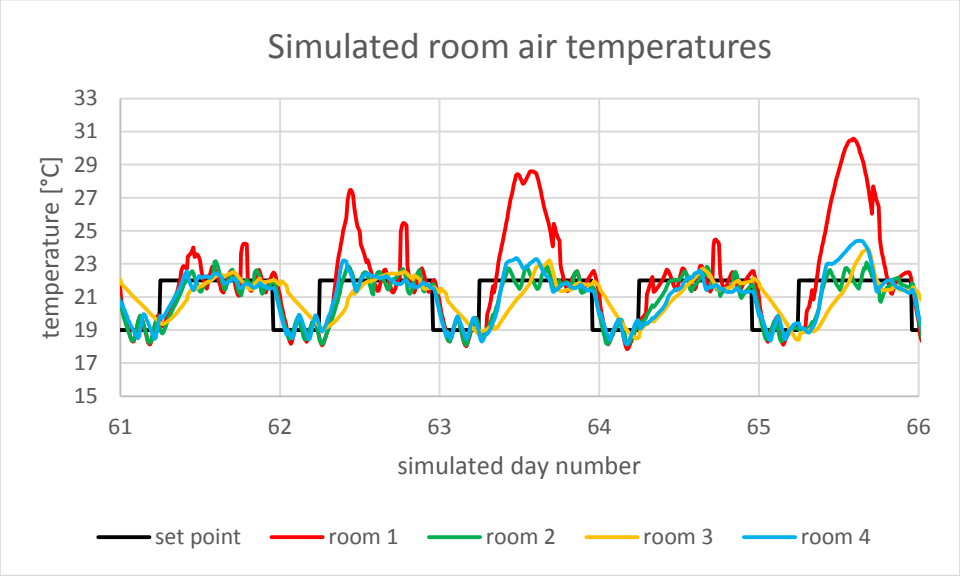

Figure 2.28. Comparison of air temperatures in the four rooms between the test rig (top) and the annual simulation program (bottom) for a five-day period of the baseline test.

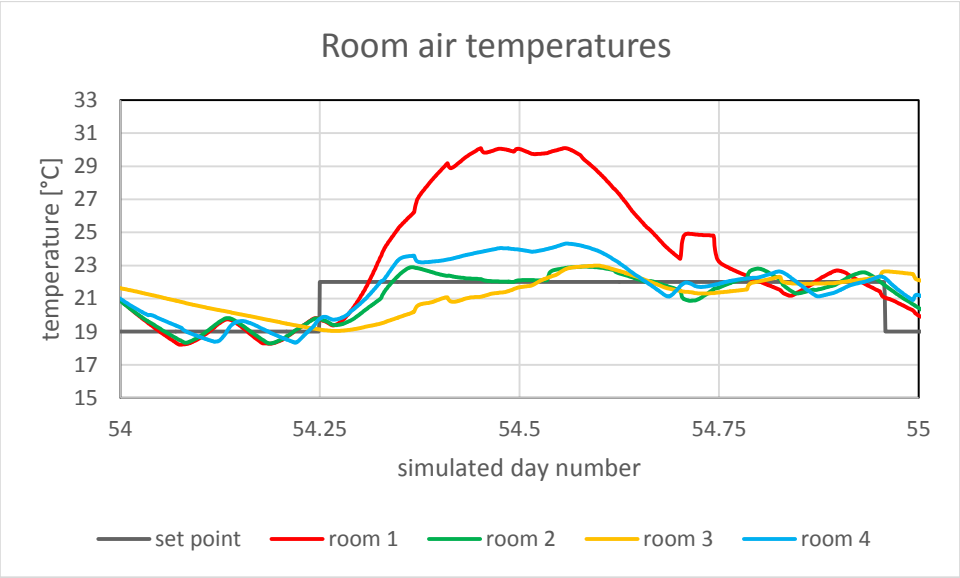

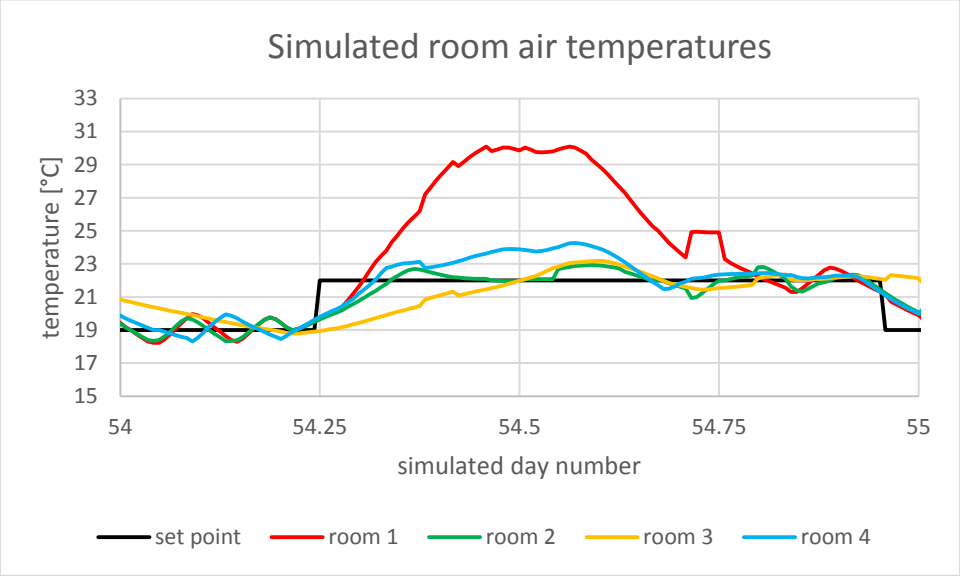

Figure 2.29. Comparison of air temperatures in the four rooms between the test rig (top) and the annual simulation program (bottom) for one day with clear sky conditions during the baseline test.

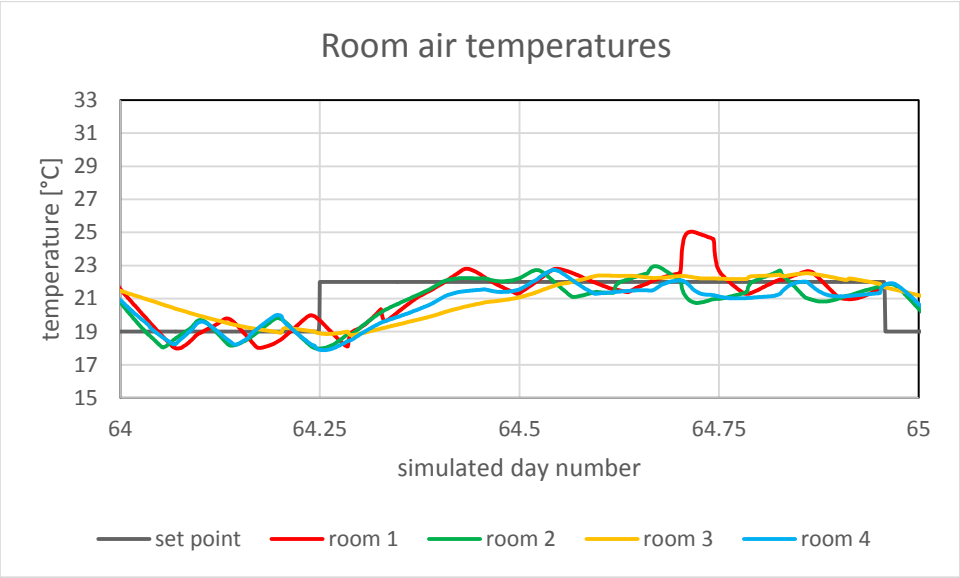

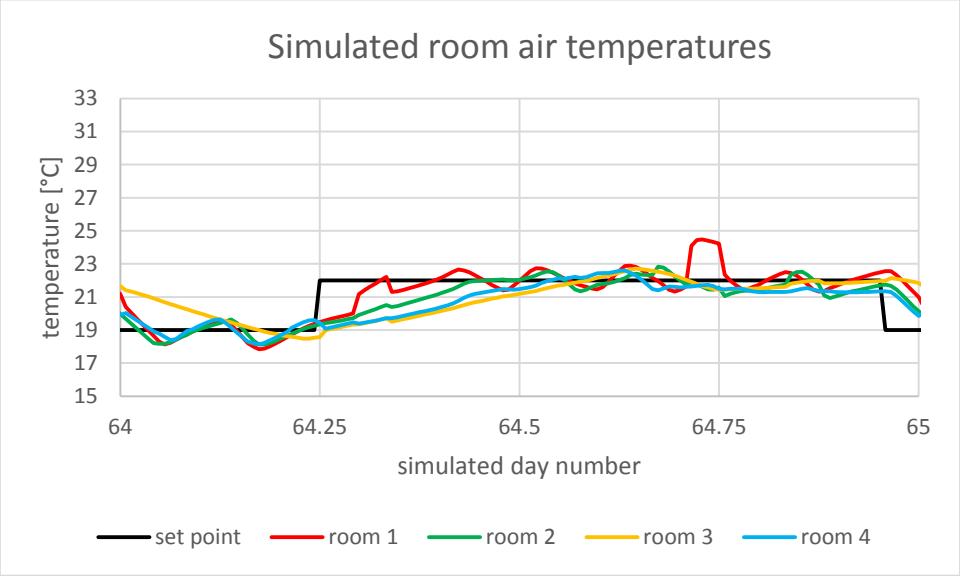

Figure 2.30. Comparison of air temperatures in the four rooms between the test rig (top) and the annual simulation program (bottom) for one day with overcast conditions during the baseline test.

Figures 2.32-34 compare the power demand of the heat pump measured at the test rig and the power demand calculated by the annual simulation program during the baseline test.

Figure 2.32 shows very different measured and calculated patterns of the power demand of the heat pump. The reason for this is that in order to speed up the annual simulation, a very simple model of the heat pump was chosen as the heat pump model of Dymola (on which the annual simulation program is based) is very complex and, therefore, until now rather slow (although the speed of the heat pump model has been increased due to the OPSYS project) – please refer to Appendix D and H for further details.

The simple model of the heat pump has been obtained from (Jensen et al, 2016). The simple heat pump model is based on test results from a different heat pump than the one situated in the test rig. These test results are shown in figure 2.31.

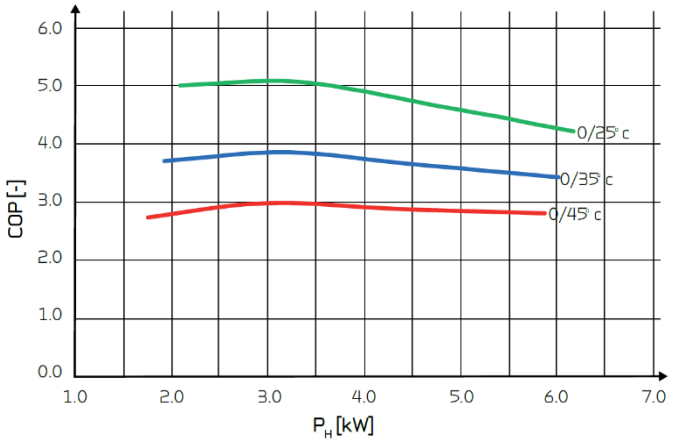

Figure 2.31. The COP of the heat pump depends on the temperature set and the heat production measured according to the test procedures stated in EN 14511. The meaning of the numbers to the right of the curves is as follows: the inlet temperature of the brine was always 0°C, while the forward temperature from the heat pump to the heating system was 25, 35 and 45°C leading to ΔTs of 25°C, 35°C and 45 K, respectively.

The values shown in figure 2.31 were measured according to the specifications given in EN 14511. In these tests, a part of the power to the brine circulation pump and the circulation pump(s) of the heating system is included in the COP, i.e. the necessary pumping energy to overcome the pressure drop across the heat pump itself. The tests have been carried out with a constant flow on each side of the heat pump. The power added to the power of the heat pump was 24 W. When using figure 2.31, the Carnot efficiency and simple multi-regression, the following equations for the heat production based on the power to the heat pump and the ΔT may be derived:

$$\Delta T = (T_h - T_c) \quad [1]$$

$$COP_{carnot} = T_h / \Delta T \quad [2]$$

$$COP_{HP} = eta * COP_{carnot} \quad [3]$$

$$eta = -0.02623*P + 0.0010993*\Delta T + 0.4016 \quad [4]$$

$$Q_H = P * COP_{HP} \quad [5]$$

where: COP_{carnot} is the system Carnot COP based on the forward temperature from the heat pump (25, 35 and 45°C) and the brine temperature to the heat pump (0°C) in figure 2.31

T_h: is the forward temperature from the heat pump [K]

T_c: is the brine inlet temperature to the heat pump [K]

COP_{HP}: is the "real" COP of the heat pump at the actual operating conditions

eta: is the system Carnot efficiency of the heat pump

P: is the electrical power to the heat pump [kW]

Q_H: (P_H in figure 2.31) is the calculated heat produced by the heat pump [kW]

The above model does not consider the thermal inertia of the heat pump, which e.g. has the result that the forward temperature - differently from the heat pump on the test rig - immediately reaches the specified value. Figure 2.32 shows that the maximum power consumption of the simple heat pump model was chosen to be 2.5 kW, while the power demand was 0.5 kW at on/off control of the heat pump as shown in figure 2.33 (day 54). The maximum power of the heat pump on the test rig seems to be 3.5 kW, while the power demand of the heat pump at on/off control at the test rig is about 1.3 kWh. Cf. the explanation under figure 2.31, the simple model only considers a part of the electricity demand of the brine and circulation pumps. Furthermore, the simple model does not include any electricity demand when the heat pump is stopped (see figures 2.33 and 2.34) – i.e. electricity to the control and the circulation pump of the heat emitting system.

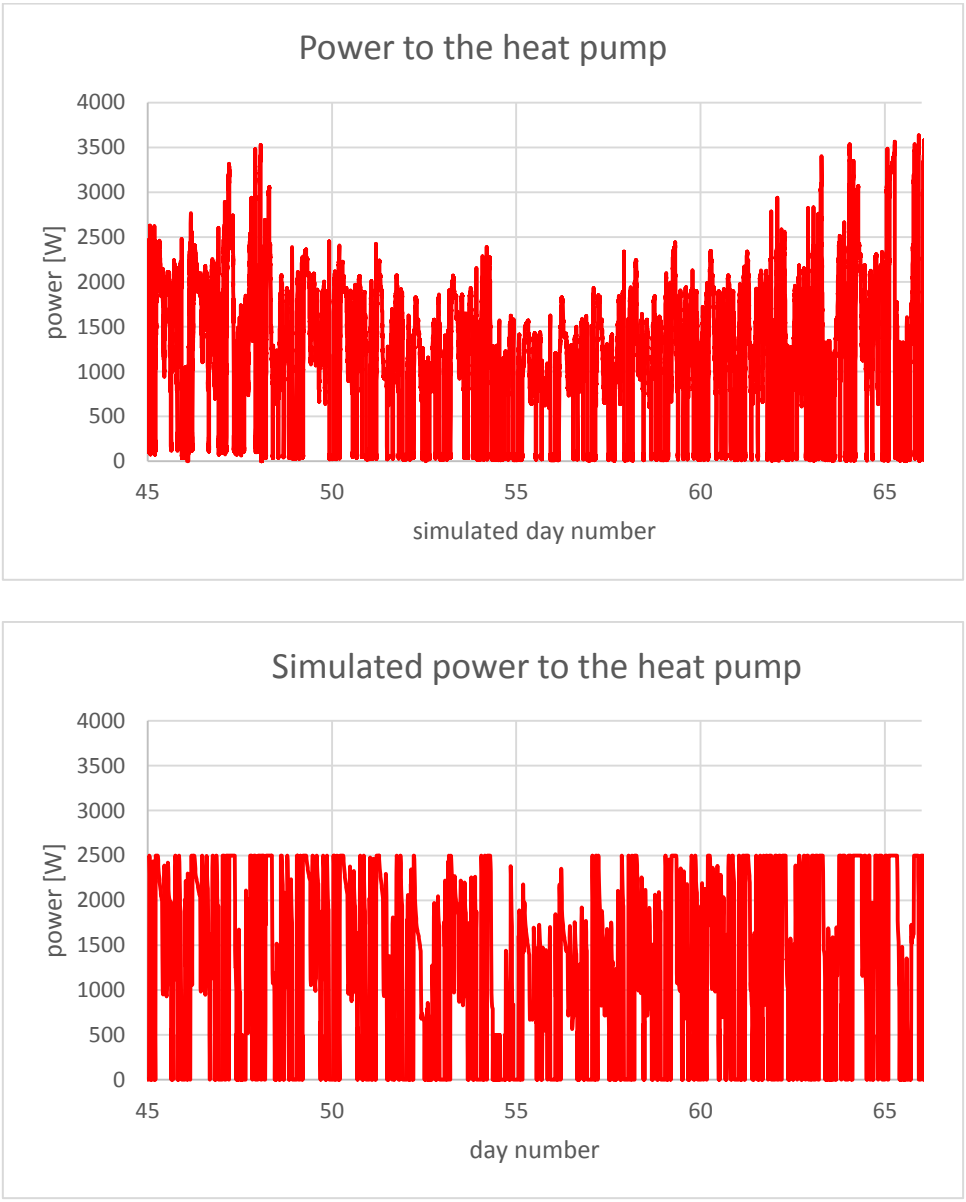

Figure 2.32. Power demand of the heat pump during the baseline test – measured on the test rig (top) and calculated by the annual simulation program (bottom).

The electricity demand of the heat pump during the baseline test was 607 kWh for the test rig while the annual simulation program calculated an electricity demand of 557 kWh

for the same period. Thus, the annual simulation underestimates the energy demand of the heat pump by 8 %. However, this difference is caused by not correctly considering the entire consumption of electricity to the pumps in the system and to the control of the heat pump. This is easy to fix in the annual simulation program. However, the above shows that there is a very good agreement between the measured and the simulated cumulated energy demand of the heat pump.

Figures 2.33 and 2.34 compare the measured and the calculated power demand of the heat pump in more details. Due to the simple model of the heat pump in the annual simulation program, the patterns of the two power demands are not identical. However, they have a recognizable common tendency.

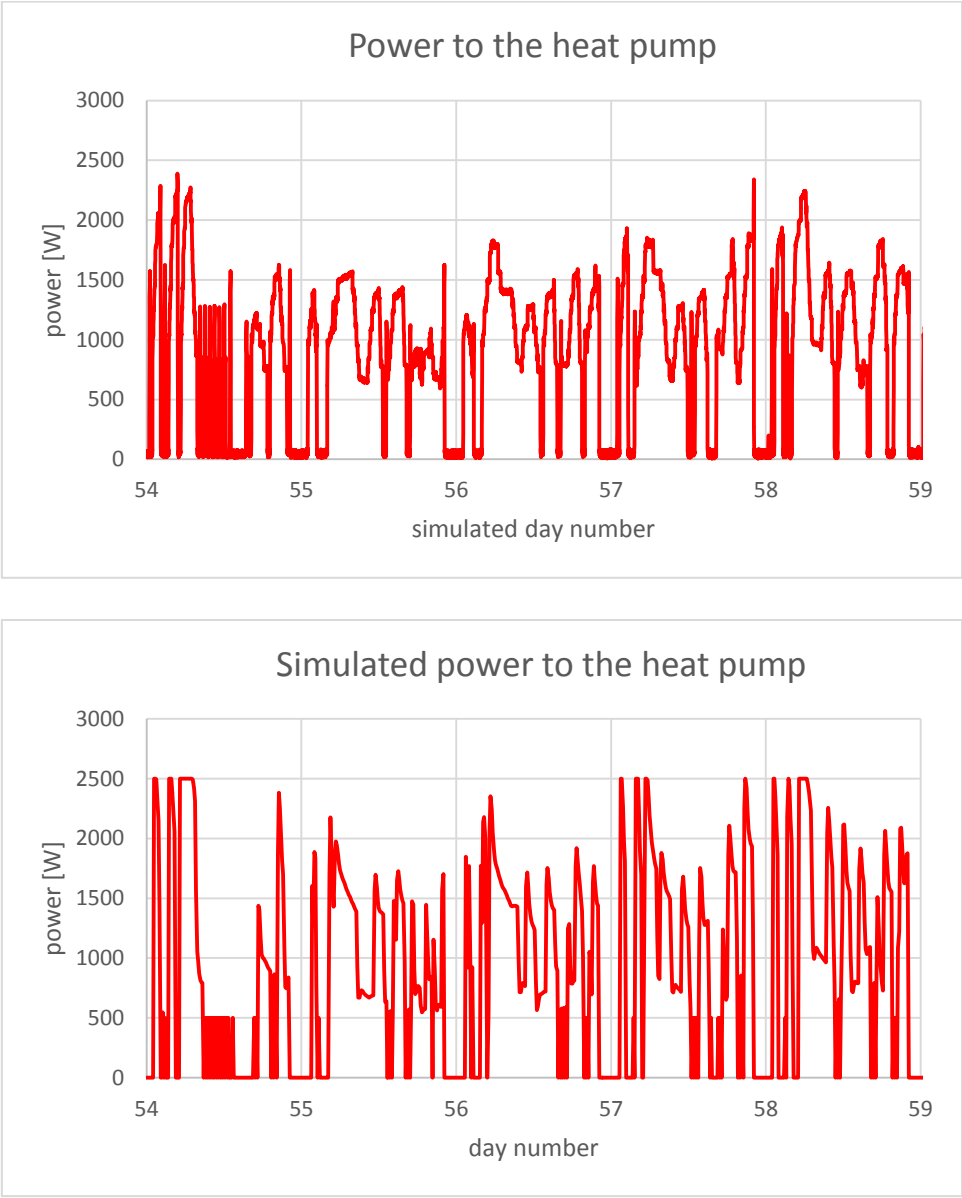

Figure 2.33. Power demand of the heat pump during the "warmest" period of the baseline test – measured on the test rig (top) and calculated by the annual simulation program (bottom).

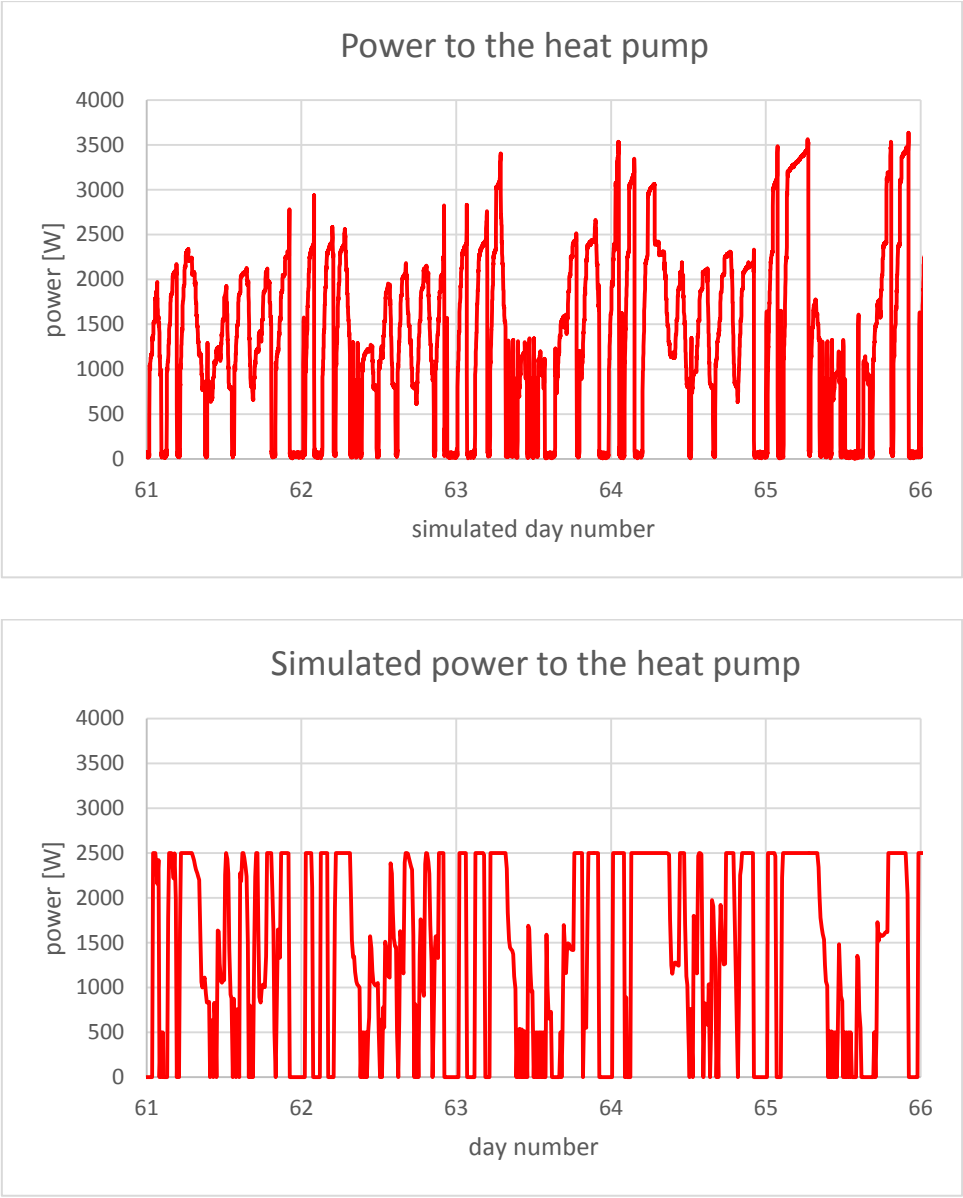

Figure 2.34. Power demand of the heat pump during the coldest period of the baseline test – measured on the test rig (top) and calculated by the annual simulation program (bottom).

The patterns of the measured and the calculated power demands of the heat pump are less close than the pattern of the air temperatures shown in figures 2.27-30. The reason for the air temperatures from the test rig and the annual simulation program being close, although the power demands are less close, is the inertia for the entire system: heat pump, underfloor heating system, and constructions of the house. There is no direct coupling between the heat produced by the heat pump and the air temperatures of the rooms. It takes time before the heat increases the temperature of the rooms, and this is further slowed down by the fact that the internal constructions of the rooms are heated up as well. The opposite occurs when the heat pump stops: it takes time for the rooms to cool down. So, as long as the heat injections (over time) are identical and happens not too far apart (dependent on the time constant of the buildings), differences in when the heat is produced by the heat pump will hardly be notices in the room air temperatures. This fact can be utilized for optimization of when heat is produced and delivered to the

rooms in order to optimize the COP of the entire system This is in fact the underlying hypothesis of the present project.

2.7 Conclusion

In the above sections, the performance of the test rig is investigated.

Firstly: it was investigated how well the test rig can obtain the conditions specified by the house model and the simulation program of the test rig pc. The investigation shows that the test rig was almost perfectly able to create the specified return temperatures from the four underfloor heating circuits. This was the main concern during the design of the test rig as it is very difficult to control the outlet temperature of a heat exchanger using PID control. Thus, achieving this nearly perfect match is a big success.

Due to the inertia of the test rig, it was of course not possible to fit the forward temperature exactly to a temperature given by a heating curve with the ambient temperature as input. However, this is also the case in real life, so here the test rig is performing as expected. It was shown that the "virtual" ambient temperature (instead of an ambient temperature sensor) given to the heat pump functions as expected. This means that the forward temperature can be manipulated by a more advanced control system, which also controls the telestats of the heating system.

The temperature of the brine has been a challenge. A buffer tank and a great amount of speculations were needed in order to obtain the not perfect, but quite good fit with the temperature of the brine specified in Appendix C – a sinus curve over the year without daily fluctuations. However, the very stable brine temperature given in Appendix C is not really seen in real life, where the brine temperature also slightly fluctuates depending on the actual running of the heat pump. Therefore, it is assessed that the test rig gives a realistic picture of this value.

The patterns of the flow rates and the air temperatures of the rooms are assessed to be very realistic. The flow rates influence each other as in real life. The decay and the increase of the air temperatures in the rooms due to the night set back seem rather realistic when considering it is a not well-insulated house from the 1970's. In addition, the influence of solar radiation, people and appliances seems to be correctly modelled.

Secondly: the measurements from the test rig were compared with the annual simulation program. Despite the many simplifications in the annual simulation program with regard to the heat pump model, the flow rates, the forward, and the brine temperatures, the comparison showed good compliance between the results from the two tools. As an example, the calculated electricity demand of the heat pump was only 8 % lower than the electricity demand measured at the test rig for the 21 days long baseline test. The main reason for the difference was that the simple model of the annual simulation program did not consider the entire amount of electricity to pumps and control in the test rig correctly.

All in all, the performed investigations leads to the conclusion that the two tool seem to perform as intended.

3 Special case

The following describes a special case where a baseline test was started, but the heat pump was for unknown reasons switched off three days into the test. The heat pump was switched on again after approximately one day. This test shows how the test rig handles such unforeseen situations. The knowledge might be utilized in special purpose cases.

Figure 3.1 shows the measured room air temperatures for the first six days of the baseline test, where the heat pump was switched off for one day, compared to a baseline test where the heat pump was not switched off. Figure 3.2 shows the ambient temperature during the same period as figure 3.1.

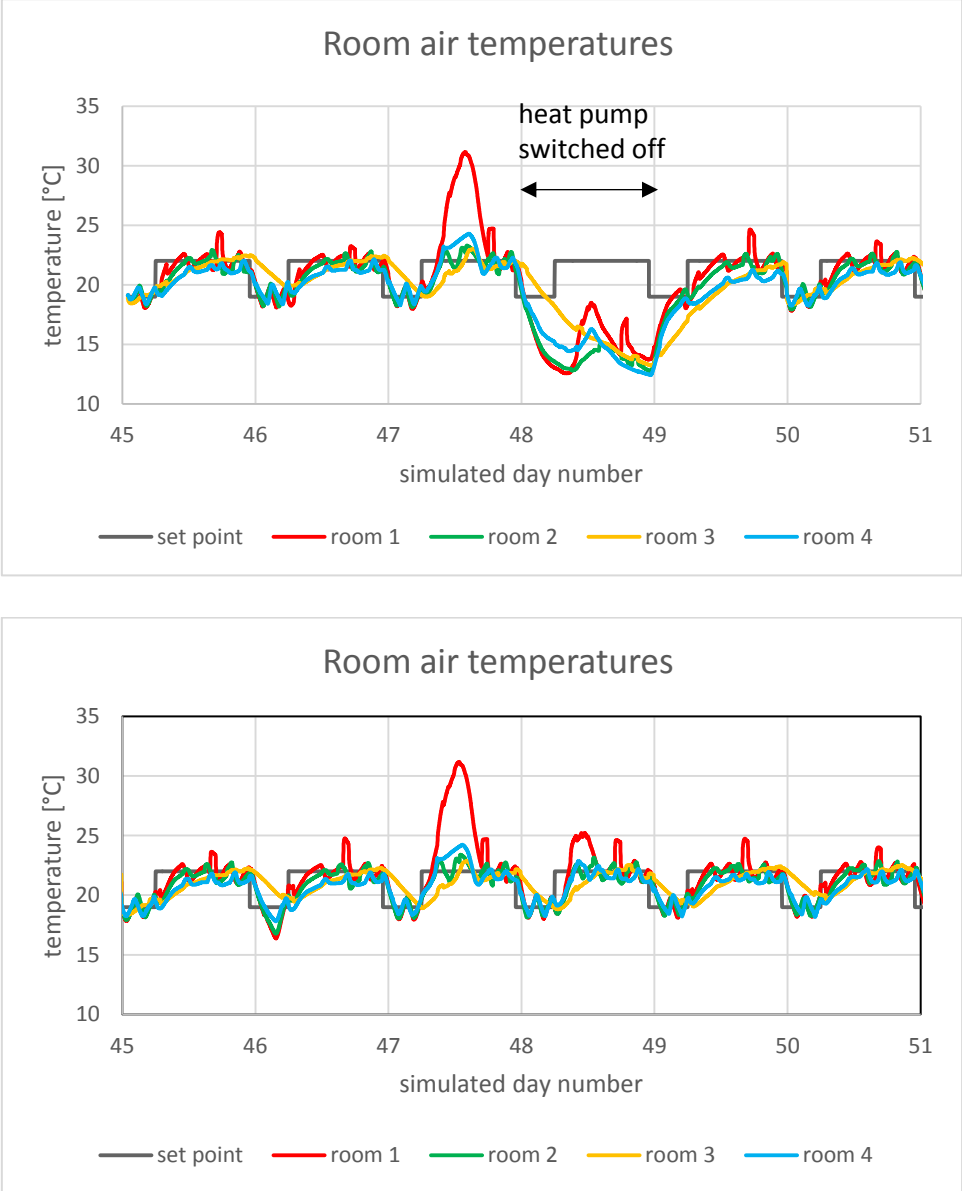

Figure 3.1. The baseline test where the heat pump was switched off for one day (top) and where the heat pump was not switched off (bottom).

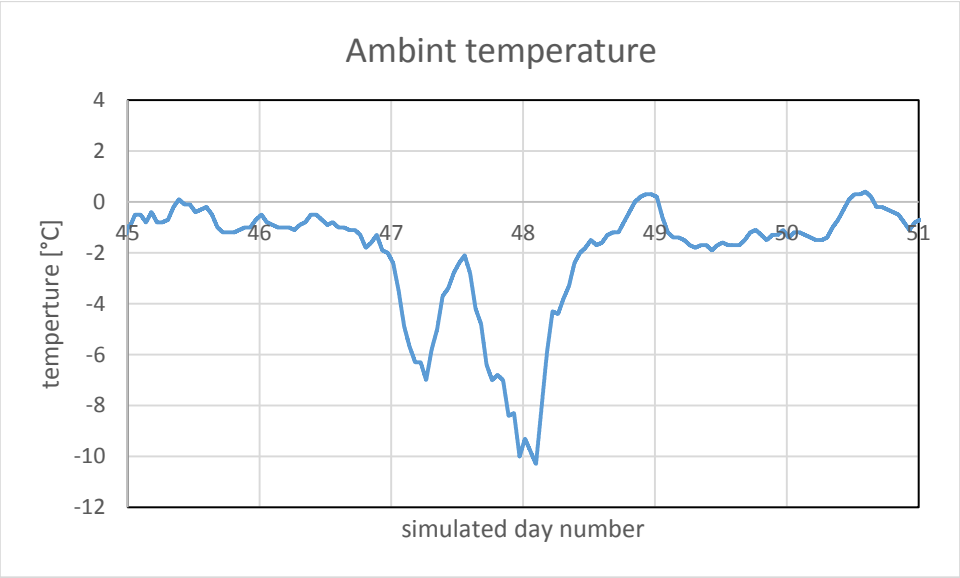

Figure 3.2. The ambient temperature during the first six days of the baseline test.

Figure 3.2 shows that the stop of the heat pump occurred during a very cold night – the ambient temperature was down to just below -10°C. Figure 3.3 shows a close-up of the day when the heat pump was switched off. Figure 3.3 shows a realistic decay of the room air temperatures. The reason for the slower decay of room 4 is that two persons sleep in this small room. The temperatures of rooms 1, 2, and 4 raise during the day due to some solar radiation. The increase of the air temperatures after the heat pump was started also seems realistic. Due to an ambient temperature between -10 and 0°C the lowest air temperature of the rooms reaches 12.5°C because the 1970's house is not well insulated.

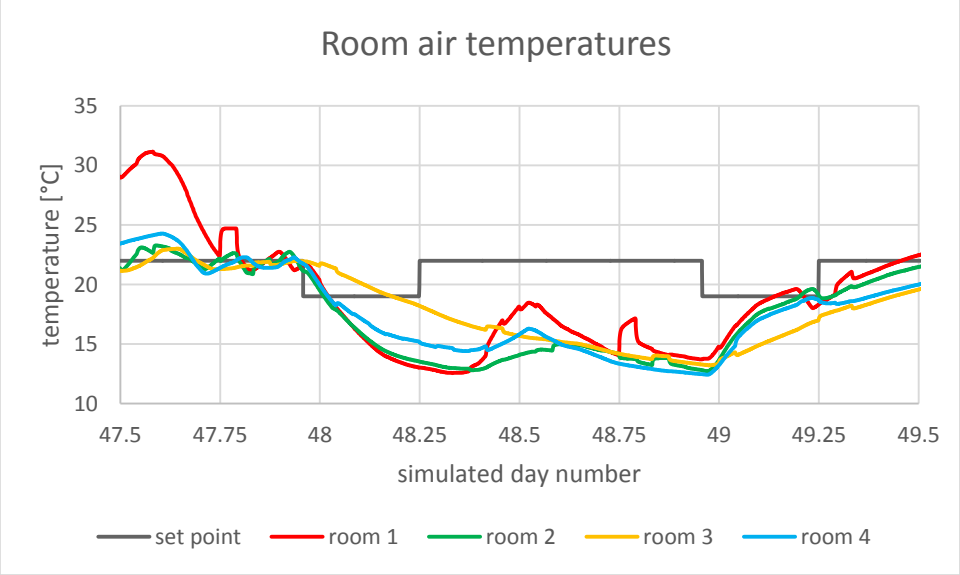

Figure 3.3. The room air temperatures during the stop of the heat pump.

Although the air temperatures of the rooms go down to 12.5°C, the room air temperatures are back to normal after one day – seen when comparing day 50 for the two cases in figure 3.1. This is also realistic for a 1970's house.

The above means that the effect of simulated breakdowns of the heat pump may be investigated. It also means that if something goes wrong during a test, normal running may quickly be restored and the test will not be completely lost. This is important, as the tests are real time. Therefore, restarting a test may lead to a great amount of lost time.

1 Conclusion

Two main tools have been developed within the OPSYS project:

- the OPSYS test rig
- a fast simulation program for carrying out annual simulations

The basis of the simulation program on the test rig and the annual simulation program is identical: a Phython script with the same house model imbedded as a FMU. The house model was developed in the programming language Dymole (Modelica). However, while the simulation program controls the test rig with a real heat pump, the annual simulation program has a virtual heat pump in the form of simple equations.

When developing new combined control strategies for heat pumps and heat emitting systems, the purpose of the two developed tools is that the annual simulation tools can be used to perform many parametric studies in order to optimize the control strategy. Once a control is designed, a special purpose test can be carried out on the test rig in order to test the control strategies in a more realistic environment, before the control strategy is demonstrated in real houses. Therefore, the rationale is:

- demonstration in real houses is of course best. However, there are so many non-controllable variables in a real house that it can be difficult to draw real significant conclusions unless the control is demonstrated in many houses. Demonstration in real houses is time consuming and very expensive
- simulation is cheap and fast, but it lacks the credibility due to the fact that all inputs and the environment are fully specified, typically in a very simple way. This may lead to conclusions, which are not possible in real life
- hardware in the loop (e.g. the OPSYS test rig) establishes a bridge between the two above described approaches. In the OPSYS test rig, some input is controllable while the environment is realistic, but repeatable as opposed to real houses

For the two tools to fulfil their purposes, it is necessary that the test rig gives realistic measurements and that the two tools give comparable results. The purpose of the present Appendix was, therefore, to investigate if:

- the test rig realistically represents the conditions in a real house
- does the two tools giver comparable results

Based on the conducted investigations, the answer to the two above questions is (until proven otherwise): yes.

Furthermore, the investigations carried out in the following Appendix G show that the test rig and the annual simulation program are capable of testing more advanced control strategies as well.

It is, therefore, concluded that the OPSYS project has succeeded in creating two valuable tools for the development of more advanced control strategies for the combination of heat pumps and heat emitting systems.

2 References

Jensen, S.Ø., Christensen, C.H., Jørgensen, D.M. and Huet, J., 2016. Smart Meter Case Study. Danish Technological Institute. Report part of the iPower Project. https://www.teknologisk.dk/ipower/39033.